Journal of the Neurological Sciences 318 (2012) 100–105

Contents lists available at SciVerse ScienceDirect

Journal of the Neurological Sciences

journal homepage: www.elsevier.com/locate/jns

Heterozygous UDP-GlcNAc 2-epimerase and *N*-acetylmannosamine kinase domain mutations in the *GNE* gene result in a less severe GNE myopathy phenotype compared to homozygous *N*-acetylmannosamine kinase domain mutations

Madoka Mori-Yoshimura [a,*], Kazunari Monma [b], Naoki Suzuki [c], Masashi Aoki [c], Toshihide Kumamoto [d], Keiko Tanaka [e], Hiroyuki Tomimitsu [f], Satoshi Nakano [g], Masahiro Sonoo [h], Jun Shimizu [i], Kazuma Sugie [j], Harumasa Nakamura [a,k], Yasushi Oya [a], Yukiko K. Hayashi [b], May Christine V. Malicdan [b], Satoru Noguchi [b], Miho Murata [a], Ichizo Nishino [b]

[a] *Department of Neurology, National Center Hospital, National Center of Neurology and Psychiatry, 4-1-1 Ogawahigashi, Kodaira, Tokyo 187-8551, Japan*
[b] *Department of Neuromuscular Research, National Institute of Neuroscience, National Center of Neurology and Psychiatry, 4-1-1 Ogawahigashi, Kodaira, Tokyo 187-8502, Japan*
[c] *Department of Neurology, Tohoku University School of Medicine, 1-1 Seiryo, Aoba-ku, Sendai 980-8574, Japan*
[d] *Department of Internal Medicine 3, Faculty of Medicine, Oita University, 1-1 Idaigaoka, Hasama, Yufu-shi, Oita 879-5593, Japan*
[e] *Department of Neurology, Kanazawa Medical University, 1-1 Daigaku, Uchinadamachi, Kahoku-gun, Ishikawa, 920-0214, Japan*
[f] *Department of Neurology and Neurological Science, Graduate School, Tokyo Medical and Dental University, Yushima 1-5-45, Bunkyo-ku, Tokyo 113-8519, Japan*
[g] *Department of Neurology, Osaka City General Hospital, 2-13-22, Miyakojimahonndoori, Miyakojima-ku, Osaka534-0021, Japan*
[h] *Department of Neurology, Teikyo University School of Medicine, Kaga 2-11-1, Itabashi-ku, Tokyo 173-8605, Japan*
[i] *Department of Neurology, Division of Neuroscience, Graduate School of Medicine, University of Tokyo, 7-3-1 Hongo, Bunkyo-ku, Tokyo 113-8655, Japan*
[j] *Department of Neurology, Nara Medical University School of Medicine, 840 Shijo, Kashihara, Nara 634-8521, Japan*
[k] *Clinical Trial Division, Division of Clinical Research, National Center Hospital of Neurology and Psychiatry, 4-1-1 Ogawahigashi, Kodaira, Tokyo 187-8551, Japan*

ARTICLE INFO

Article history:
Received 10 January 2012
Received in revised form 20 March 2012
Accepted 21 March 2012
Available online 14 April 2012

Keywords:
GNE myopathy
Distal myopathy with rimmed vacuoles
Hereditary inclusion body myopathy
Glucosamine (UDP-N-acetyl)-2-epimerase/*N*-acetylmannosamine kinase
(UDP-N-acetyl)-2-epimerase domain
N-acetylmannosamine kinase domain
Questionnaire
Natural history

ABSTRACT

Background: Glucosamine (UDP-N-acetyl)-2-epimerase/*N*-acetylmannosamine kinase (GNE) myopathy, also called distal myopathy with rimmed vacuoles (DMRV) or hereditary inclusion body myopathy (HIBM), is a rare, progressive autosomal recessive disorder caused by mutations in the *GNE* gene. Here, we examined the relationship between genotype and clinical phenotype in participants with GNE myopathy.
Methods: Participants with GNE myopathy were asked to complete a questionnaire regarding medical history and current symptoms.
Results: A total of 71 participants with genetically confirmed GNE myopathy (27 males and 44 females; mean age, 43.1 ± 13.0 (mean ± SD) years) completed the questionnaire. Initial symptoms (*e.g.*, foot drop and lower limb weakness) appeared at a mean age of 24.8 ± 8.3 years. Among the 71 participants, 11 (15.5%) had the ability to walk, with a median time to loss of ambulation of 17.0 ± 2.1 years after disease onset. Participants with a homozygous mutation (p.V572L) in the *N*-acetylmannosamine kinase domain (KD/KD participants) had an earlier disease onset compared to compound heterozygous participants with mutations in the uridine diphosphate-N-acetylglucosamine (UDP-GlcNAc) 2-epimerase and *N*-acetylmannosamine kinase domains (ED/KD participants; 26.3 ± 7.3 vs. 21.2 ± 11.1 years, respectively). KD/KD participants were more frequently non-ambulatory compared to ED/KD participants at the time of survey (80% vs. 50%). Data were verified using medical records available from 17 outpatient participants.
Conclusions: Homozygous KD/KD participants exhibited a more severe phenotype compared to heterozygous ED/KD participants.

1. Introduction

Glucosamine (UDP-N-acetyl)-2-epimerase/*N*-acetylmannosamine kinase (GNE) myopathy, also known as distal myopathy with rimmed vacuoles (DMRV), Nonaka myopathy (MIM: 605820) or hereditary inclusion body myopathy (HIBM; MIM: 600737), is an early adult-onset, progressive myopathy that affects the tibialis anterior muscle, but spares quadriceps femoris muscles [1,2]. The disease is caused by a mutation in the *GNE* gene, which encodes a bifunctional enzyme [uridine diphosphate-*N*-acetylglucosamine (UDP-GlcNAc) 2-epimerase (GNE) and *N*-acetylmannosamine kinase (MNK)] known to catalyze two rate-limiting reactions involved in cytosolic sialic acid synthesis [3–7]. Mutations in the *GNE* gene result in decreased enzymatic activity *in vitro* by 30–90% [7–10]. Therefore, hyposialylation is thought to

* Corresponding author. Tel.: +81 42 341 2711; fax: +81 42 346 1852.
E-mail address: yoshimur@ncnp.go.jp (M. Mori-Yoshimura).

0022-510X/$ - see front matter © 2012 Elsevier B.V. All rights reserved.
doi:10.1016/j.jns.2012.03.016

contribute to the pathogenesis of GNE myopathy. This is supported by the myopathic phenotype associated with a mouse model expressing the human D176V mutant GNE protein (GNE−/−hGNED176V-Tg) [11]. Muscle atrophy and weakness are prevented by oral treatment with sialic acid metabolites in this mouse model [12].

A phase I clinical trial using oral sialic acid therapy has recently been performed in Japan for the treatment of GNE myopathy (ClinicalTrials.gov; NCT01236898). A similar phase I study is currently underway in the United States (ClinicalTrials.gov; NCT01359319). Natural history and genotype–phenotype correlations need to be established for a successful phase II clinical trial for the treatment of GNE myopathy. However, only a small number of studies have been conducted that review the natural course of this disease. In addition, the presence of genotype–phenotype correlations is controversial in GNE myopathy, with most reports denying significant correlations [7]. In fact, substantial heterogeneity is observed among participants who have the same mutations. For example, few subjects with p.D176V and p.M712T mutations exhibited a normal or very mild phenotype, with disease onset after the age of 60 [3,13]. Furthermore, only a limited number of studies that analyze compound heterozygous patients are available. Nonetheless, such studies report a variable degree of severity [14–17].

To clarify the potential relationship between genotype and clinical phenotype (*i.e.*, age at onset, disease course, and current symptoms) of GNE myopathy, we performed a questionnaire-based survey of participants with confirmed GNE myopathy.

2. Participants and methods

2.1. Study population

We obtained approval for this study from the Medical Ethics Committee of the National Center of Neurology and Psychiatry (NCNP). Seventy-eight participants with known GNE myopathy were seen at 8 hospitals specializing in muscle disorders in Japan and 83 participants (not all genetically diagnosed) from the Participants Association for Distal Myopathies (PADM) were recruited. Participants provided written informed consent prior to completing the questionnaire.

A total of 75 participants completed and returned the questionnaire. Of the 75 participants analyzed, 4 were found to have only one heterozygous mutation. Because single heterozygous mutations have not been confirmed to cause GNE myopathy, these 4 participants were excluded from this study.

2.2. Study design

The present study is a retrospective and cross-sectional analysis, which includes 71 participants with genetically confirmed GNE myopathy. Clinical information was collected from participants using a questionnaire and genetic information was acquired from available medical records.

2.3. Questionnaire

Participants completed a self-reporting questionnaire regarding 1) developmental and past symptoms, 2) past and present ambulatory status, and 3) information about diagnosis and medical services (Supplementary material, original version in Japanese).

To determine developmental history, we collected the following information: 1) trouble before and/or during delivery, 2) body weight and height at birth, 3) age at first gait, 4) exercise performance during nursery, kindergarten, or school, and 5) age at onset and signs of first symptoms. Participants were also asked about the onset of 1) gait disturbance, 2) walking with assistance (*i.e.*, cane and/or orthotics and/or handrails), 3) wheelchair use, 4) loss of ambulation, and 5) current gait performance. With regard to medical history, participants were asked about 1) age at the time of first hospital visit, 2) whether or not they had symptoms at the time of visit, 3) age at the time of final diagnosis, 4) how many hospitals/clinics were visited before final diagnosis, and 5) whether a biopsy was performed.

2.4. Medical record examination

To verify the accuracy of the information provided by each participant, available medical records from 17 participants (23.9%) seen at outpatient clinics at NCNP were examined (9 males and 8 females).

2.5. Data handling and analysis

All variables were summarized using descriptive statistics, which included mean, standard deviation (SD), median, range, frequency, and percentage. Each variable was compared against age, sex, genotype, and domain mutation (*i.e.*, within the UDP-GlcNAc 2-epimerase domain: ED or *N*-acetylmannosamine kinase domain: KD). Student's *t* test was used to compare the means for each participant group (ED/ED, ED/KD and KD/KD participants). Data from the two participant groups were calculated using chi-square contingency table analysis. The time from disease onset to walking with assistance, time from disease onset to wheelchair use, and time from disease onset to loss of ambulation were evaluated using the Kaplan–Meier method with log-rank analysis. Questionnaire reliability was tested using intraclass correlation coefficients (ICCs), and two-sided 95% confidence intervals (CIs) were calculated using a one-way random effects analysis of variance model for inter-rater reliability. All analyses were performed using SPSS for Macintosh (version 18, SPSS Inc., Chicago, IL).

3. Results

3.1. General characteristics

A total of 71 Japanese individuals (27 males and 44 females) participated in the study. The mean age at data collection was 43.1 ± 10.7 years. None of the participants showed developmental abnormalities during infancy or early childhood.

3.2. GNE mutations

Forty-one percent of study participants (n = 29/71) had homozygous mutations, while 59% (n = 42/71) had compound heterozygous mutations (Table 1). Among homozygous participants, 86.2% (n = 25/29) harbored the p.V572L mutation, while the remaining participants had other mutations. No homozygous participants for the p.D176V mutation were identified. Among compound heterozygous participants, 28.5% (n = 12/42) had p.D176V/p.V572L mutations, while the remaining participants had other mutations. With respect to allelic frequency, 50.0% (71/142) were p.V572L, 20.4% (29/142) p.D176V, 3.5% (5/142) p.C13S, 2.8% (4/142) p.M712T, and 2.1% (3/142) p.A630T. All other mutations accounted for 2%. A total of 18.3% (n = 13/71) of participants were homozygous with a mutation in the GNE domain (ED/ED), 39.4% (n = 28/71) of participants were compound heterozygous with a mutation in the GNE domain and one in the MNK domain (ED/KD), and 42.3% (n = 30/71) of participants had a mutation in the MNK domain in both alleles (KD/KD).

3.3. Past and present symptoms

Mean participant age at symptom onset was 25.2 ± 9.2 years (range, 12–58 years; median, 24.5 years). There was no significant difference between males and females for current age, age at disease

Table 1
Genotypes of the GNE myopathy patient population.

		Questionnaire	Outpatients
ED/ED	Total	13	4
	Homozygote	1	0
	p.C13S homozygote	1	
	Compound heterozygote	12	4
	p.C13S/p.M29T	1	1
	p.C13S/p.A631	1	1
	p.D176V/p.F233S	1	1
	p.D176V/p.R306Q	2	
	p.R129Q/p.D176V	1	
	p.R129Q/p.R277C	1	
	p.D27L/p.D176V	1	1
	p.B89S/p.D176V	1	
	p.D176V/p,R246W	1	
	p.D176V/p.R321C	1	
	p.D176V/p.V331A	1	
ED/KD	Total	28	8
	Compound heterozygote	28	8
	p.D176V/p.V572L	12	3
	p.C13S/p.V572L	1	1
	p.D176V/p.I472T	1	1
	p.D176V/p.L603F	1	1
	p.R177C/p.V572L	1	1
	383insT/p.V572L	1	1
	p.D176V/p.G708S	2	
	p.D187G/p.V572L	2	
	p.R8X/p.V572L	1	
	p.D176V/p.G568S	1	
	p.D176V/p.H626R	1	
	p.D176V/p.A630T	1	
	p.I276T/p.V572L	1	
	p.G295D/p.A631V	1	
	p.A600E/p.D176V	1	
KD/KD	Total	30	5
	Homozygote	28	5
	p.V572L homozygote	25	4
	p.M712T homozygote	2	
	p.A630T homozygote	1	
	Compound heterozygote	2	0
	p.V572L/p.R420X	1	1
	1756Gdel (stop)/p.V572L	1	

onset, age at walking with assistance, age at wheelchair use, and current ambulatory status. Initial symptoms included gait disturbance (66.2%, n = 47/71), other lower limb symptoms (26.8%, n = 19/71), easily fatigued (23.9%, n = 17/71), and weakness of hands and fingers (8.5%, n = 6/71). In addition, 21.1% (n = 15/71) had onset of symptoms before the age of 20. When specifically asked, 47.8% (n = 34/71) described themselves as slow runners during childhood, and 42.5% reported having had difficulty with physical exercise during school years.

3.4. Diagnosis

Mean participant age at diagnosis was 33.9 ± 12.6 years (median, 29.5 years; range 17 to 67 years). Mean participant age at first physician visit was 29.6 ± 10.4 years (median, 27 years; range, 12–62 years), and mean time between first visit and diagnosis was 4.4 ± 8.3 years.

3.5. Walking with assistance and wheelchair use

At the time of the survey, 52.0% (n = 37/71) were ambulant (41.3 ± 12.8 years); however, only 15.5% (n = 11/71, 40.0 ± 13.6 years) could walk without assistance, with the remaining 35.2% requiring assistance (n = 25/71; 41.8 ± 12.7 years). Only 7.0% of these participants (n = 5/71) could walk up stairs, while 49.3% (n = 35/71) were non-ambulant. Wheelchairs were used by 63.6% (23.9% partially bound and 43.7% totally bound) and an electric wheelchair was used by 41.9% (n = 31/71). Mean participant age of wheelchair users was 34.9 ± 11.7 years (range, 18–70 years). Wheelchairs were not used by 32.4% (n = 26/71) of participants. Current age of wheelchair-free participants was 39.4 ± 12.3 years (range, 21–61 years; median, 34 years) and that of wheelchair-bound participants was 42.8 ± 12.6 years (range, 21–71; median, 42 years).

Kaplan–Meier analysis revealed a median proportional age at walking with assistance of 30.0 ± 1.4 years. Median proportional age of wheelchair users was 36.0 ± 2.7 years, and that for loss of ambulation was 45.0 ± 4.2 years. The time from disease onset to walking with assistance was 7.0 ± 0.4 years, time from disease onset to wheelchair use was 11.5 ± 1.2 years, and time from disease onset to loss of ambulation was 17.0 ± 2.1 years.

3.6. Correlation between disease genotype and phenotype

To determine if a correlation between genotype and phenotype existed, we compared domain mutations (ED/KD, or both) available from medical reports to questionnaire answers (Table 2). Participants with KD/KD mutations (both homozygous and heterozygous) were younger and more severely affected compared to participants with ED/KD or ED/ED mutations. No significant difference in current age or age at disease onset between ED/ED and ED/KD participants was identified. Kaplan–Meier analyses revealed that the proportional time from disease onset to wheelchair use and from disease onset to loss of ambulation was significantly shorter in KD/KD compared to ED/KD participants. ED/ED participants exhibited a shorter time of disease onset to wheelchair use compared to ED/KD participants (Table 3, Fig. 1).

3.7. Comparison between p.V572L homozygous and p.D176V/p.V572L compound heterozygous participants

To compare clinical features in patients with the same mutations, we specifically analyzed data from those with p.V572L (n = 25/71, 35.2%) and p.D176V/p.V572L (n = 12/71, 16.9%) mutations, as these two were the most frequent mutations in our study population (Table 2). Age at disease onset of homozygous participants (p.V572L) was 21.3 ± 5.7 years (range, 12–32 years) and time from disease onset to wheelchair use was 11.3 ± 5.4 years (range, 3–21 years). Only 16.0% (n = 4/25) of these homozygous participants reported that they were not currently using a wheelchair. In contrast, the mean age at disease onset of heterozygous participants (p.D176V/p.V572L) was 35.5 ± 14.1 years (range, 13.5–57 years) and time from disease onset to wheelchair use was 17.9 ± 7.0 years (range, 11–28 years). A total of 66.7% of these compound heterozygous participants (n = 8/12) reported that they were not using a wheelchair.

3.8. Questionnaire response compared to medical records

Questionnaires from 17 participants (NCNP outpatient participants) were compared to available medical records (Table 2). Age at disease onset, age at onset of gait disturbance, age at walking with assistance, and age at loss of ambulation were assessed for inter-rater reliability. Age at disease onset, age at onset of gait disturbance, age at walking with assistance, and age at loss of ambulation were assessed for inter-rater reliability. ICC values were 0.979 (95% CI 0.941–0.992) for age at disease onset, 0.917 (95% CI 0.752–0.972) for age at onset of gait disturbances, 0.985 (95% CI 0.949–0.995) for age at walking with assistance, and 0.967 (95% CI 0.855–0.993) for age at loss of ambulation.

4. Discussion

The present study provides a detailed overview of disease severity and progression in 71 Japanese participants with genetically confirmed GNE myopathy. Questionnaire-based surveys have been used to study

Table 2
Comparison of disease course among genotypes.

		Total	ED/ED	ED/LD	KD/KD
Questionnaire	*n*	71	13	28	30
	Age (years old)	43.1 ± 10.7	44.2 ± 11.2	45.3 ± 13.4	40.6 ± 13.0
	Age at onset (years old)	25.5 ± 9.2	26.3 ± 7.3[†]	29.8 ± 11.0[*]	21.2 ± 5.5[*,†]
	Age at walking with assistance	31.8 ± 10.0	34.0 ± 11.1	35.6 ± 10.9[*]	27.8 ± 6.8[*]
	Duration from onset to walking with assistance	8.4 ± 6.5	7.5 ± 7.3	9.2 ± 6.5	8.0 ± 6.6
	Wheelchair user (%)	48 (67.8)	10(76.9)	14 (50.0)[*]	24 (80.0)[*]
	Wheelchair use since (age)	37.6 ± 8.6	36.4 ± 12.0	43.0 ± 8.7[*]	31.2 ± 9.3[*]
	Number of patients with lost ambulation	35 (49.8)	6(46.2)	8 (28.6)[*]	21 (70.0)[*]
	Age at lost ambulation	33.6 ± 9.2	31.2 ± 6.0	39.7 ± 9.5	32.1 ± 9.3
	Duration from onset to loss of ambulation	12.2 ± 5.2	9.8 ± 3.5	13.8 ± 6.4	12.4 ± 5.1
NCNP outpatients	*n*	17	4	8	5
	Age (years old)	43.9 ± 14.1	53.5 ± 8.9[†]	44.3 ± 16.3	35.6 ± 9.2[†]
	Age at onset (years old)	25.8 ± 9.2	33.4 ± 9.2[†]	29.6 ± 13.5	19.6 ± 4.2[†]
	Duration from onset to walking with assistance	7.5 ± 4.2	8.9 ± 5.1	8.1 ± 4.7	5.2 ± 1.5
	Wheelchair user (%)	12 (70.6)	3 (75.0)	4 (50.0)	4 (100)
	Wheelchair use since (age)	33.3 ± 12.6	47.5 ± 17.7	35.2 ± 12.4	25.8 ± 6.3
	Number of patients with lost ambulation	9 (52.9)	3 (75.0)	3 (28.6)[*]	5 (100)[*]
	Age at lost ambulation	33.8 ± 9.3	40.0 ± 0.0	39.0 ± 16.5	31.0 ± 8.2
	Duration from onset to loss of ambulation	10.7 ± 4.2	11.2 ± 5.6	11.1 ± 7.8	6.2 ± 2.6

In the questionnaire group, age at onset and age at walking with assistance were significantly younger in KD/KD patients than in ED/KD patients. The number of wheelchair users and patients with loss of ambulation was significantly higher in the KD/KD group than in the ED/KD group. In contrast, with the exception of age at onset, there were no significant differences between ED/ED and ED/KD or KD/KD patients in these clinical parameters. The ED/ED patients were older than the others, and KD/KD patients tended to show the fastest progression.

* $p<0.05$ between ED/KD and KD/KD.

† $p<0.05$ between ED/ED and KD/KD.

the natural disease course of other rare neuromuscular disorders, such as Pompe disease [18] and spinal muscular atrophy type-1 [19]. It is difficult to establish the natural history of such rare disorders using medical records only because patients are typically seen in many different hospitals. In the present study, we used a self-reporting questionnaire and support its use for complementing medical records because it provides a more complete disease overview and establishes specific clinical trends or correlations. Indeed, our questionnaire demonstrates excellent inter-rater reliability against medical records and yields several findings regarding differences in disease progression among genetically distinct, GNE myopathy participants.

Only 15.5% of participants could walk and 7.0% could walk up stairs without assistance, which reflects the fact that GNE myopathy patients often require canes and/or leg braces at an early disease stage. This indicates that traditional six-minute walk or four-step walking tests often used to evaluate muscular dystrophies or myopathies can only be applied in a very limited number of cases, such as natural disease course studies or clinical trials. Therefore, alternate evaluation tools are required, which should include functional measurements that can be completed without canes or braces. For example, the Gross Motor Function Measure is a useful tool for evaluating mildly and severely affected patients [20].

The male to female ratio in our study population (27 males and 44 females) was skewed from the expected ratio for autosomal recessive inheritance. However, the male to female ratio of the 17 NCNP outpatient participants was 9:8. One possible explanation for the observed sex ratio in our study population is that female participants tend to be more enthusiastic toward questionnaire-based and/or PADM activities. There was no significant difference in age at survey and age at disease onset between male and female participants. However, in a mouse model of GNE myopathy, weight loss and muscle atrophy were more pronounced and occurred earlier in females compared to males [11].

We showed that KD/KD mutations are associated with a more severe phenotype compared to ED/KD mutations. Indeed, KD/KD participants had an earlier disease onset, a more rapid and progressive disease course, and a shorter time from disease onset to loss of ambulation. This was also observed in the 17 NCNP outpatient participants analyzed in our study. In contrast, ED/ED participants did not show significant differences across disease course parameters analyzed except for an earlier and later age at disease onset compared to ED/KD and KD/KD participants, respectively. Thus, ED/ED participants appear to have a disease severity intermediate between ED/KD and KD/KD participants. One possible explanation is that the major mutation, p.V572L, may be associated with a more severe phenotype. In general, the reasons for this earlier onset and disease progression remain unknown. Jewish GNE myopathy patients with homozygous p.M712T mutations have a milder phenotype compared to Japanese patients, as most of their quadriceps are spared and they usually become wheelchair-bound 15 years or more after disease onset [13,21]. Our study population included two women with homozygous p.M712T mutations: a 38 year-old ambulant and a 35 year-old non-ambulant participant. Although the two participants had a slightly later disease onset (ages 23 and 27 years, respectively) compared to KD/KD participants, the difference was not significant.

An asymptomatic patient with a p.D176V homozygous mutation was previously reported [3]. The study suggested that p.D176V homozygous patients may show a mild or late disease onset phenotype. The results presented here may support this observation as no p.D176V homozygous participants were present in our study

Table 3
Inter-rater reliability of the questionnaire.

	Onset	Age of gait disturbance	Age of gait with help	Age at loss of ambulant
Number of patients	17	17	13	9
ICC (95% CI)	0.979 (0.941–0.992)	0.917 (0.752–0.972)	0.985 (0.949–0.995)	0.967 (0.855–0.993)
p	0.000	0.000	0.000	0.000

Age at onset, age at onset of gait disturbances, age at walking with assistance, and age at loss of ambulation were assessed in a subgroup of 17 outpatients to evaluate the inter-rater reliability of the questionnaire.

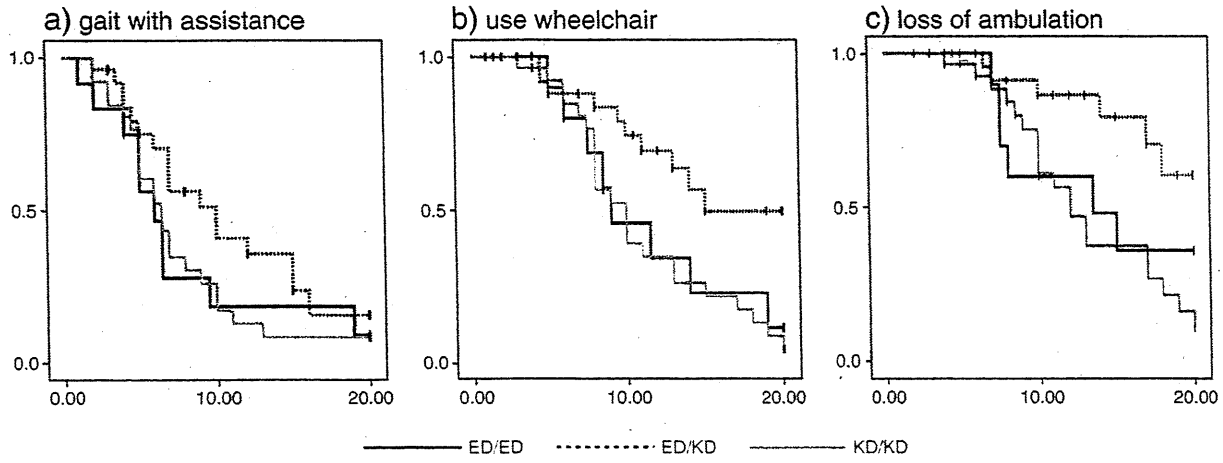

Fig. 1. Kaplan–Meier analysis of time from disease onset to (a) walking with assistance, (b) wheelchair use, and (c) loss of ambulation. Significant differences between ED/KD and KD/KD genotypes were identified. Age at disease onset was significantly different between ED/ED participants and ED/KD and KD/KD participants.

population, although p.D176V was the second most common mutation carried by 29 of our participants. In addition, a high variability was observed regarding age at disease onset and disease progression, underscoring the role of a yet-to-be identified factor(s) in determining disease phenotype.

The recruitment of participants from PADM and highly specialized neurology hospitals is a potential source of selection bias and thus a limitation of this study. These participants are likely to be more motivated because they are more severely affected compared to the general patient population. Furthermore, patients with lower disease severity may not yet be diagnosed with GNE myopathy. Therefore, our study may not accurately reflect the general patient population. Nevertheless, we believe our findings provide important information as our study population covers a broad range in age (22 to 81 years) and symptoms (minimal to wheelchair-bound). Finally, recall bias may also affect results presented in this retrospective study. Therefore, future studies should be performed with an emphasized prospective design.

In conclusion, our study shows that the KD/KD genotype (*i.e.*, p.V572L homozygous mutation) is associated with a more severe phenotype compared to compound heterozygous ED/KD mutations. Because only a small number of participants could walk, future studies should include ambulation-independent motor tests to yield a more comprehensive clinical overview in GNE myopathy patients with different genotypes.

Supplementary data to this article can be found online at doi:10.1016/j.jns.2012.03.016.

Conflict of interest

We certify that there is no conflict of interest with any financial organization regarding the material discussed in the manuscript.

Acknowledgments

We thank members of the Patients Association for Distal Myopathies (PADM) for their help. This work was partly supported by the Research on Intractable Diseases of Health and Labor Sciences Research Grants; Comprehensive Research on Disability Health and Welfare Grants, Health and Labor Science Research Grants; Intramural Research Grant (23-4, 23-5) for Neurological and Psychiatric Disorders of NCNP; and a Young Investigator Fellowship from the Translational Medical Center, NCNP.

References

[1] Nonaka I, Sunohara N, Satoyoshi E, Terasawa K. Yonemoto K. Autosomal recessive distal muscular dystrophy: a comparative study with distal myopathy with rimmed vacuole formation. Ann Neurol 1985;17:51–9.
[2] Argov Z, Yarom R. "Rimmed vacuole myopathy" sparing the quadriceps. A unique disorder in Iranian Jews. J Neurol Sci 1984;64:33–43.
[3] Nishino I, Noguchi S, Murayama K, Driss A, Sugie K, Oya Y, et al. Distal myopathy with rimmed vacuoles is allelic to hereditary inclusion body myopathy. Neurology 2002;59:1689–93.
[4] Eisenberg I, Avidan N, Potikha T, Hochner H, Chen M, Olender T, et al. The UDP-N-acetylglucosamine 2-epimerase/N-acetylmannosamine kinase gene is mutated in recessive hereditary inclusion body myopathy. Nat Genet 2001;29:83–7.
[5] Kayashima T, Matsuo H, Satoh A, Ohta T, Yoshiura K, Matsumoto N, et al. Nonaka myopathy is caused by mutations in the UDP-N-acetylglucosamine-2-epimerase/N-acetylmannosamine kinase gene (GNE). J Hum Genet 2002;47:77–9.
[6] Keppler OT, Hinderlich S, Langner J, Schwartz-Albiez R, Reutter W, Pawlita M. UDP-GlcNAc 2-epimerase: a regulator of cell surface sialylation. Science 1999;284:1372–6.
[7] Malicdan MC, Noguchi S, Nishino I. Recent advances in distal myopathy with rimmed vacuoles (DMRV) or hIBM: treatment perspectives. Curr Opin Neurol 2008;21:596–600.
[8] Noguchi S, Keira Y, Murayama K, Ogawa M, Fujita M, Kawahara G, et al. Reduction of UDP-N-acetylglucosamine 2-epimerase/N-acetylmannosamine kinase activity and sialylation in distal myopathy with rimmed vacuoles. J Biol Chem 2004;279:11402–7.
[9] Broccolini A, Gidaro T, De Cristofaro R, Morosetti R, Gliubizzi C, Ricci E, et al. Hyposialylation of neprilysin possibly affects its expression and enzymatic activity in hereditary inclusion–body myopathy muscle. J Neurochem 2008;105:971–81.
[10] Salama I, Hinderlich S, Shlomai Z, Eisenberg I, Krause S, Yarema K, et al. No overall hyposialylation in hereditary inclusion body myopathy myoblasts carrying the homozygous M712T GNE mutation. Biochem Biophys Res Commun 2005;328:221–6.
[11] Malicdan MC, Noguchi S, Nonaka I, Hayashi YK, Nishino I. A Gne knockout mouse expressing human GNE D176V mutation develops features similar to distal myopathy with rimmed vacuoles or hereditary inclusion body myopathy. Hum Mol Genet 2007;16:2669–82.
[12] Malicdan MC, Noguchi S, Hayashi YK, Nonaka I, Nishino I. Prophylactic treatment with sialic acid metabolites precludes the development of the myopathic phenotype in the GNE myopathy mouse model. Nat Med 2009;15:690–5.
[13] Argov Z, Eisenberg I, Grabov-Nardini G, Sadeh M, Wirguin I, Soffer D, et al. Hereditary inclusion body myopathy: the Middle Eastern genetic cluster. Neurology 2003;60:1519–23.
[14] Tomimitsu H, Shimizu J, Ishikawa K, Ohkoshi N, Kanazawa I, Mizusawa H. Distal myopathy with rimmed vacuoles (DMRV): new GNE mutations and splice variant. Neurology 2004;11:1607–10.
[15] Yabe I, Higashi T, Kikuchi S, Sasaki H, Fukazawa T, Yoshida K, et al. GNE mutations causing distal myopathy with rimmed vacuoles with inflammation. Neurology 2003;12:384–6.
[16] Chu CC, Kuo HC, Yeh TH, Ro LS, Chen SR, Huang CC. Heterozygous mutations affecting the epimerase domain of the GNE gene causing distal myopathy with rimmed vacuoles in a Taiwanese family. Clin Neurol Neurosurg 2007;109:250–6.
[17] Ro LS, Lee-Chen GJ, Wu YR, Lee M, Hsu PY, Chen CM. Phenotypic variability in a Chinese family with rimmed vacuolar distal myopathy. J Neurol Neurosurg Psychiatry 2005;76:752–5.

[18] Hagemans ML, Winkel LP, Van Doorn PA, Loonen MC, Hop WJ, Reuser AJ, et al. Clinical manifestation and natural course of late-onset Pompe's disease in 54 Dutch patients. Brain 2005;128:671–7.
[19] Oskoui M, Levy G, Garland CJ, Gray JM, O'Hagen J, De Vivo DC, et al. The changing natural history of spinal muscular atrophy type 1. Neurology 2007;69: 1931–6.
[20] Sienko Thomas S, Buckon CE, Nicorici A, Bagley A, McDonald CM, Sussman MD. Classification of the gait patterns of boys with Duchenne muscular dystrophy and their relationship to function. J Child Neurol 2010;25:1103–9.
[21] Eisenberg I, Grabov-Nardini G, Hochner H, Korner M, Sadeh M, Bertorini T, et al. Mutations spectrum of GNE in hereditary inclusion body myopathy sparing the quadriceps. Hum Mutat 2003;21:99.

SCIENTIFIC REPORTS

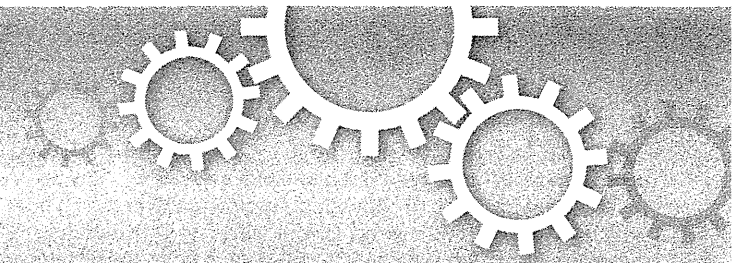

OPEN

SUBJECT AREAS:
RNA SPLICING
RNA
HIGH-THROUGHPUT SCREENING
DRUG DISCOVERY

Received
8 February 2013

Accepted
17 May 2013

Published
5 July 2013

Correspondence and requests for materials should be addressed to S.I. (cishiura@mail.ecc.u-tokyo.ac.jp)

Manumycin A corrects aberrant splicing of *Clcn1* in myotonic dystrophy type 1 (DM1) mice

Kosuke Oana[1], Yoko Oma[1], Satoshi Suo[1], Masanori P. Takahashi[2], Ichizo Nishino[3], Shin'ichi Takeda[4] & Shoichi Ishiura[1]

[1]Department of Life Sciences, Graduate School of Arts and Sciences, The University of Tokyo, Komaba, Tokyo, Japan, [2]Department of Neurology, Osaka University Graduate School of Medicine, Suita, Osaka, Japan, [3]Department of Neuromuscular Research, National Institute of Neuroscience, National Center of Neurology and Psychiatry, Kodaira, Tokyo, Japan, [4]Department of Molecular Therapy, National Institute of Neuroscience, National Center of Neurology and Psychiatry, Kodaira, Tokyo, Japan.

Myotonic dystrophy type 1 (DM1) is the most common muscular dystrophy in adults and as yet no cure for DM1. Here, we report the potential of manumycin A for a novel DM1 therapeutic reagent. DM1 is caused by expansion of CTG repeat. Mutant transcripts containing expanded CUG repeats lead to aberrant regulation of alternative splicing. Myotonia (delayed muscle relaxation) is the most commonly observed symptom in DM1 patients and is caused by aberrant splicing of the skeletal muscle chloride channel (*CLCN1*) gene. Identification of small-molecule compounds that correct aberrant splicing in DM1 is attracting much attention as a way of improving understanding of the mechanism of DM1 pathology and improving treatment of DM1 patients. In this study, we generated a reporter screening system and searched for small-molecule compounds. We found that manumycin A corrects aberrant splicing of *Clcn1* in cell and mouse models of DM1.

Myotonic dystrophy (DM), a genetic disorder, is the most common type of muscular dystrophy in adults[1]. The types of DM disease[2], DM types 1 (DM1) and 2 (DM2), differ genetically but are similar clinically. DM1 is caused by expansion of a CTG repeat in the 3′-untranslated region (UTR) of the DM protein kinase (*DMPK*) gene, whereas DM2 is caused by expansion of a CCTG repeat in intron 1 of the zinc finger 9 (*ZNF9*) gene[3–5]. DM1 presents with a variety of symptoms, such as myotonia, progressive muscle wasting, cataracts, insulin resistance, and intellectual deficits[1,6]. Identification of the DM2 mutation[5] and studies using DM1 mice that express the expanded CUG repeat[7] suggest that RNA gain-of-function causes the DM1 phenotype.

How does nucleotide expansion within a non-coding region cause DM1? An investigation of the molecular mechanism of DM1 proposed that expanded repeat RNA transcripts form hairpin structures that retain nuclear foci in DM1 cells[8], and affect the function of RNA-binding proteins[9–12]. 'Muscleblind-like' (MBNL) and 'CUGBP and ETR-3 like factor' (CELF) proteins are well-studied RNA-binding proteins. Sequestration of MBNL1 by toxic expanded RNA transcripts[11,13] and up-regulation of CUGBP-1[14] result in aberrant regulation of alternative splicing events in DM1[2]. Our previous studies indicated aberrant regulation of *MYOM1* and *PDLIM3* in DM1 patients[15,16]; more than 25 genes have been found to be misregulated in patients with DM[17]. Missplicing of the following genes has been associated with DM1 symptoms: *CLCN1*, which results in myotonia[7,18], *BIN1*, which is associated with T-tubule alterations and muscle weakness[19], and *INSR*, which contributes to insulin resistance[20]. However, there is no evident relationship between additional misspliced genes and DM1 symptoms. Therefore, further studies are needed to elucidate this association.

Myotonia is one of the features observed most commonly in individuals with DM1. People with myotonia are unable to relax certain muscles after use. For example, a person may not be able to release their grip on a doorknob or handle. In DM1 patients, the inclusion of alternative exons 6B and/or 7A, and retention of intron 2 of *CLCN1*, are observed due to aberrant regulation of alternative splicing[18]. Abnormal splicing of *CLCN1* results in a frameshift and produces premature termination codons in transcripts, leading to nonsense-mediated mRNA decay (NMD) or the production of a truncated protein with a dominant-negative effect[21]. A mouse model of DM1 expressing an expanded CUG repeat (HSA^{LR}) also shows increased inclusion of *Clcn1* exon 7A and displays

myotonia[7]. Our previous study using a *Clcn1* minigene identified regulation of exon 7A by MBNL and CELF proteins[22].

The identification of small-molecule compounds that correct missplicing events in DM1 would benefit both our understanding of novel aspects of DM1 pathogenesis and DM1 therapy. In DM1, there may be other key players in addition to MBNL and CELF. There are several approaches to DM1 therapy, such as overexpression of MBNL1[23], RNA interference targeting CUG repeat transcripts[24], inhibition of MBNL1 sequestration through use of a CAG oligonucleotide that binds to the CUG repeats[25] or a small molecule[26], and degradation of expanded CUG repeat transcripts through the RNase H pathway, which occurs through induction of 2′ methoxyethyl (MOE) gapmers[27]. Although use of an antisense oligonucleotide showed remarkable effects, there was a difficulty with body-wide delivery while small-molecule compounds have the advantage of oral formulation.

In this study, we established a Clcn1-L minigene reporter assay and found that manumycin A corrects abnormal splicing of *Clcn1*. Furthermore, we confirmed that injection of manumycin A corrects missplicing of *Clcn1* in a mouse model of DM1 via H-Ras pathway.

Results

Generation of the Clcn1-L reporter assay system. To identify small chemical compounds effective against aberrant splicing of *CLCN1* in DM1, we generated a minigene reporter vector containing the mouse *Clcn1* gene from exons 6 to 7 and the firefly luciferase gene (Fig. 1a). As shown in Fig. 1b, luciferase expression was obtained upon exclusion of exon 7A; however, inclusion of exon 7A produced a termination codon, resulting in a lack of luciferase expression. Next, we confirmed the co-transfection of Clcn1-L and DMPK constructs harboring either CTG18 (DM18) or interrupted CTG480 (DM480) repeats. RT-PCR analysis revealed that inclusion of exon 7A was significantly increased upon co-expression of Clcn1-L and DM480 compared to co-expression with DM18 (Fig. 1c,d). According to the luciferase analysis, co-expression of Clcn1-L and DM18 displayed a higher activity than did co-expression with DM480 (Fig. 1e). Note that we did not delete the initiation codon of luciferase gene. It is possible that an extra ATG codon in the Clcn1-L might induce translation of luciferase irrespective of exon 7A exclusion. However, in our experiments, the luciferase activity decreased when DM480 was transfected (Fig. 1e). Therefore, we concluded that this reporter system was properly working.

Identification of small-molecule compounds that correct aberrant splicing of Clcn1 under the expression of expanded CUG repeats in vitro. The ICCB Known Bioactives Library is a collection of compounds with defined biological activities. The library was screened to identify compounds that corrected aberrant splicing of *Clcn1* using our luciferase reporter assay. Because expanded CUG repeat expression causes aberrant regulation of alternative splicing in DM1, we transfected C2C12 cells with both the Clcn1-L luciferase reporter vector and DM480, which expresses the expanded CUG repeat. Although most compounds showed little effect compared to that of DMSO treatment (control, Table S1), some of the compounds showed high luciferase activity (Fig. S1), and Ro 31-8220, AGC, and manumycin A caused little toxicity to cells (Fig. S2). Since Ro 31-8220 was well studied with DM1[28] and AGC caused large SEM, manumycin A was chosen in this study for further analysis. Manumycin A (20 μM) showed high luciferase activity in the presence of the expanded CUG repeat (Fig. 2a and Fig. S1).

Next, we performed RT-PCR analysis to investigate whether manumycin A corrects aberrant *Clcn1* splicing caused by expression of the expanded CUG repeats. Results from RT-PCR showed that the addition of manumycin A effectively corrects aberrant splicing of *Clcn1* in the presence of the expanded CUG repeat (Fig. 2b,c). Percentages of *Clcn1* exon 7A inclusion showed that manumycin A treatment rescued abnormal exon 7A inclusion levels caused by expression of the expanded CUG repeat to levels similar to those for the normal CUG repeat (Fig. 2c). Additionally, we tested the dosage of manumycin A (~10-40 μM), and found that the effects of manumycin A were concentration-dependent (Fig. S3). High-dosage manumycin A rescued aberrant splicing in the presence of the expanded CUG repeat and showed skipping of exon 7A (Fig. S3) compared to the control (Fig. 2c).

Manumycin A corrects aberrant splicing of Clcn1 in a mouse model of DM1. Next, we examined the ability of manumycin A to rescue aberrant splicing of *Clcn1* in a mouse model (HSA^{LR}) of DM1, in which 250 CUG repeats are expressed under the control of the actin promoter. RT-PCR analysis showed elevated inclusion of *Clcn1* exon 7A in the HSA^{LR} mice compared with the wild-type mice (Fig. 3a,b). Injection of manumycin A induced a remarkable reduction in *Clcn1* exon 7A inclusion (Fig. 3c,d). However, manumycin A did not rescue aberrant splicing of *Serca1* and m-Titin (Fig. S4).

H-Ras regulates alternative splicing of Clcn1 exon 7A. Manumycin A is an antibiotic generated by *Streptomyces parvulus*[29]. It acts as a selective and vigorous inhibitor of Ras farnesyltransferase[30]. After translation, Ras protein requires several modifications: isoprenylation, proteolysis, methylation and palmitoylation[31–33]. Isoprenylation by the enzyme farnesyltransferase (FTase) or geranylgeranyltransferase I (GGTase I) is the first step in the post-translational modification of Ras. Farnesylation or geranylgeranylation is necessary for Ras to attach to the inner side of the plasma membrane. Without attachment to the cell membrane, Ras is unable to be activated[34]. H-Ras, K-Ras and N-Ras are the members of the Ras family. It is important that H-Ras is only farnesylated, whereas K-Ras and N-Ras can be farnesylated and geranylgeranylated. Thus, inhibitors of farnesyltransferase are effective in reducing the activity of H-Ras but not that of K-Ras and N-Ras[35]. Correction of *Clcn1* splicing by manumycin A may therefore be due to the inhibition of H-Ras activity. To test this possibility, we knocked down endogenous H-Ras expression using small interfering RNA (siRNA) and examined the effect of H-Ras inhibition on *Clcn1* splicing. We confirmed the efficacy of the siRNA in modulating the expression of the H-Ras by Western blot analysis (Fig. 4a). RT-PCR analysis showed reduced inclusion of *Clcn1* exon 7A in the presence of expanded CUG repeats (Fig. 4b,c). We also examined the effects of K-Ras and N-Ras knockdown and found that N-Ras knockdown reduced the inclusion of *Clcn1* exon 7A, whereas K-Ras knockdown did not alter *Clcn1* splicing (Fig. S5). Additionally, we tested whether expanded CUG repeats altered the expression levels of H-Ras. Although there was no significant difference between DM18- and DM480-transfected C2C12 cells, an upward trend was observed when cells were transfected with DM480 (Fig. S6).

Discussion

Misregulation of alternative splicing is a characteristic feature of DM1. Although the number of missplicing events is over 25, few genes have been reported to play a role in disease manifestations. Abnormal regulation of alternative splicing in the *CLCN1* gene is one of the events that can account for myotonia, which is often recognized in DM1. In this investigation, we generated a Clcn1-L reporter assay system and searched for small-molecule compounds that affect abnormal splicing of *Clcn1* in the presence of expanded CUG repeats. We found that manumycin A corrects aberrant splicing of *Clcn1*, which was confirmed *in vivo*. We also revealed that H-Ras was involved in the regulation of alternative splicing of *Clcn1* exon 7A.

Injection of DM1 model mice with manumucin A corrected aberrant splicing of *Clcn1*; however, splicing of *Serca1* and m-Titin, which

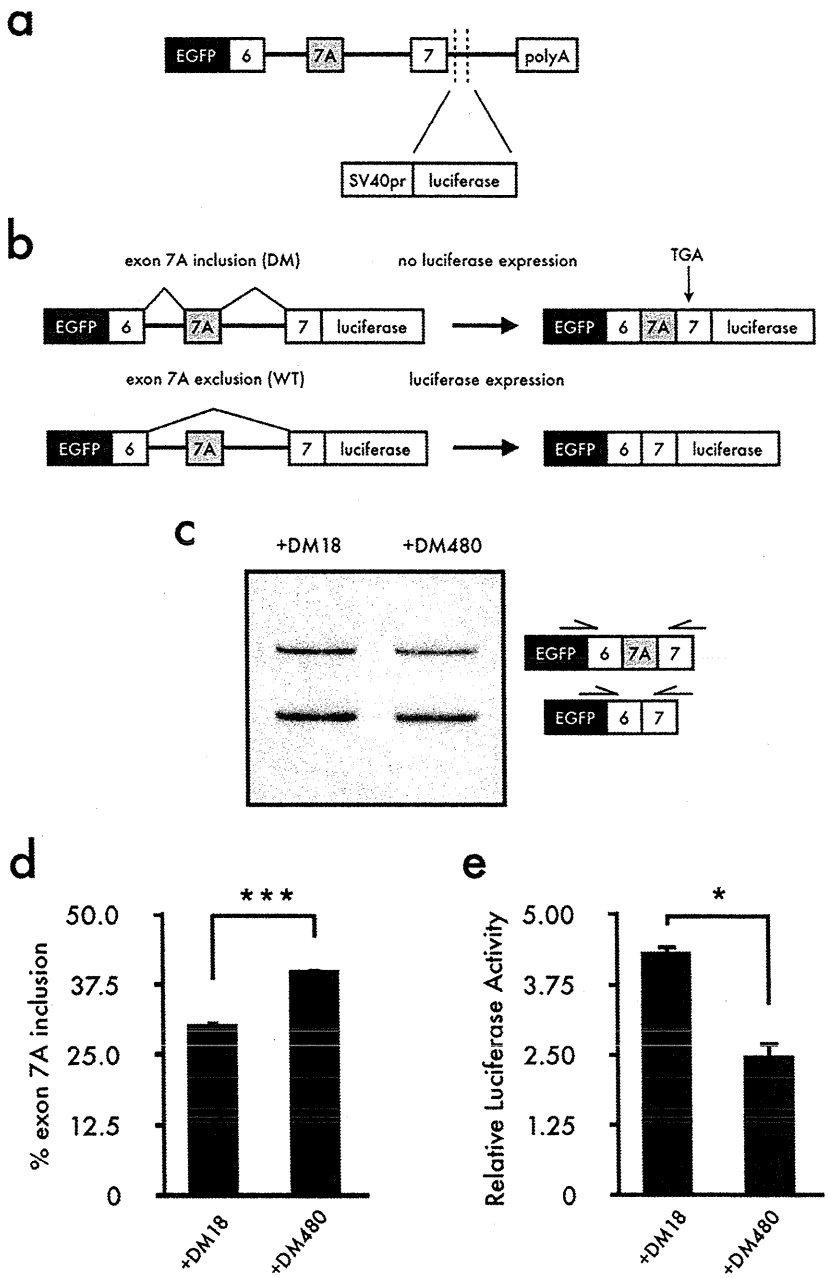

Figure 1 | Construction of the Clcn1-L reporter minigene and effect of triplet repeat expansion on the reporter vector Clcn1-L. (a) Schematic structure of the Clcn1-L minigene reporter. A genomic segment of mouse *Clcn1* containing exons 6 to 7 (including the intron) was sub-cloned downstream of EGFP in the pEGFP-C1 plasmid. Firefly luciferase was inserted in-frame with a correct *Clcn1* splicing pattern. (b) Schematic of how Clcn1-L functions. Exon 7A exclusion results in luciferase expression to detect correct *Clcn1* splicing. (c) Inclusion of *Clcn1* exon 7A increased upon expression of the expanded CUG repeat. (d) Bar charts show the quantified percentages of exon 7A inclusion (mean + SEM, n = 4). (e) Luciferase analysis showed that relative luciferase activity decreased upon expression of the expanded CUG repeat (mean + SEM, n = 3). The gel image was cropped around the region of interest and the samples (n = 4) were resolved in the same gel. Statistical significances were determined using *t*-tests (*$p < 0.05$, ***$p < 0.001$).

is also abnormally regulated in DM1[36,37], was not changed. It has been reported that *Serca1* is regulated by MBNL1[37,38] and CUGBP1[39] and that m-Titin is also regulated by MBNL1[37]. Furthermore, the expression of MBNL1 and CUGBP1 was not altered by treatment with manumycin A (Fig. S7). For these reasons, we conclude that manumycin A did not alter *Clcn1* splicing through effects on MBNL1 and CUGBP1. How, then, does manumycin A correct *Clcn1* missplicing? Manumycin A is an inhibitor of Ras farnesyltransferase, and it could inhibit Ras activity. In this study, we demonstrated that H-Ras knockdown reduced the inclusion of *Clcn1* exon7A, indicating that H-Ras is involved in a regulation of *Clcn1* splicing.

Ras proteins perform functional roles in a large number of biological processes, leading to changes in cell morphology, survival, apoptosis, and gene expression[40]. Because Ras is positioned as the central molecular switch of these biological outcomes, it must interact with a variety of downstream targets. Recent studies implicated the Ras signaling pathway in alternative splicing regulation[41]. Activation of the Ras-PI3-kinase-PKB/Akt pathway alters the

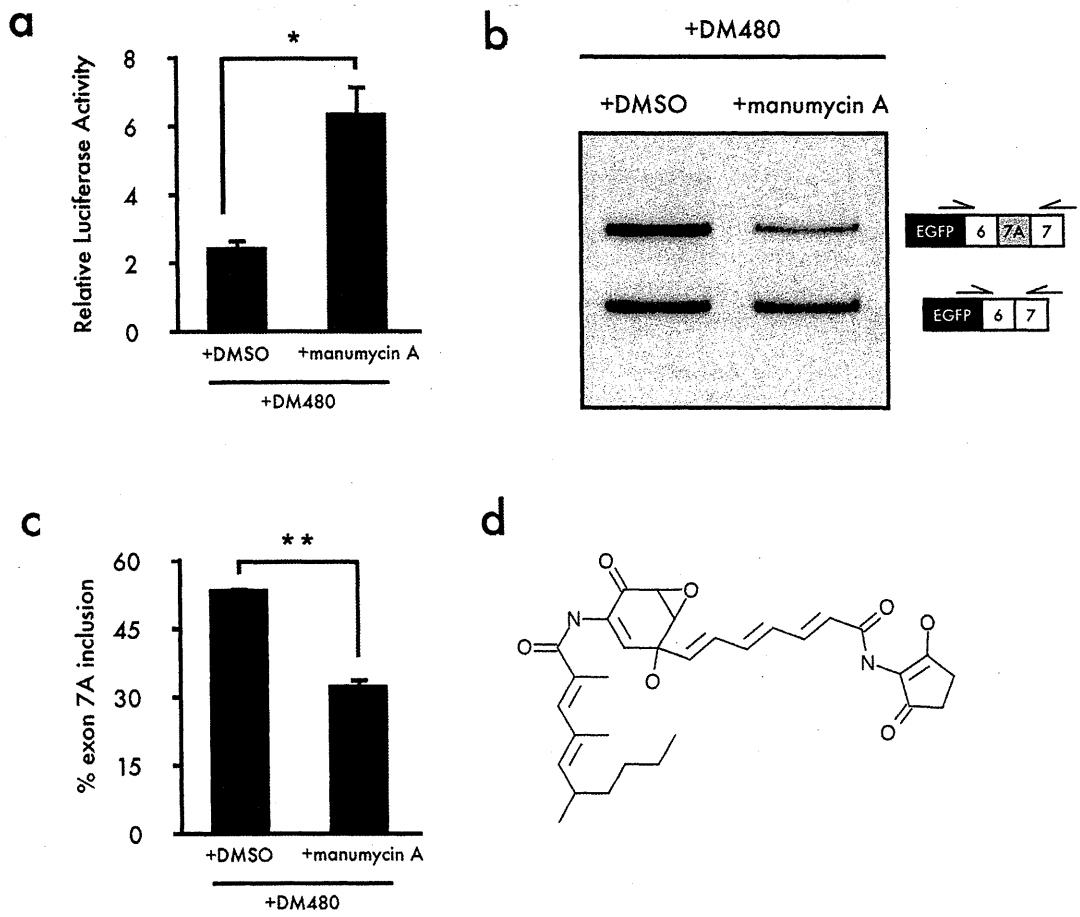

Figure 2 | Identification of small-molecule compounds that correct aberrant splicing of *Clcn1*. (a) A luciferase reporter assay showed that manumycin A corrected aberrant splicing in the presence of the expanded CUG repeat (mean + SEM, n = 3). (b) Cellular splicing analysis showed that manumycin A corrects aberrant splicing of *Clcn1*. (c) Quantification of the results shown in (b) (mean + SEM, n = 3). (d) Structure of manumycin A. The gel image was cropped around the region of interest and the samples (n = 3) were resolved in the same gel. Statistical significance was determined using *t*-tests (*$p < 0.05$, **$p < 0.01$).

phosphorylation level of the serine/arginine-rich (SR) proteins SF2/ASF and 9G8[42]. SR proteins are the best-characterized splicing regulatory factors, and it is well known that the activity of SR proteins is dependent on their phosphorylation level. Furthermore, the Ras-Raf-MEK-ERK pathway, another Ras pathway, is known to modulate alternative splicing[41,43].

Considering these studies, it is possible that manumycin A inhibits H-Ras activity and alters the H-Ras signaling pathway, resulting in correction of *Clcn1* splicing. Therefore, modulation of H-Ras signaling may influence a *trans*-acting factor other than MBNL1 and CUGBP1 and thereby contribute to *Clcn1* splicing. The effect of manumycin A is illustrated in Figure 5, although the question remains as to what kind of *trans*-acting factor is influenced by manumycin A and H-Ras. Importantly, manumycin A treatment showed reduced total amount of *Clcn1* mRNAs (with and without exon 7A) (Fig. 2b and Fig. 3c). Therefore, it is possible that manumycin A has another effect on either transcription or stability of *Clcn1* pre-mRNA.

A recent study revealed that oncogenic mutated H-Ras G12V inhibits muscle differentiation[44]. If H-Ras is involved in DM pathology, it may help us to better understand DM1. Interestingly, manumycin A only slightly changes the splicing of *Clcn1* in the absence of DM480 expression (Fig. S8). Furthermore, transfection of C2C12 cells with the expanded CUG repeat tended to increase H-Ras expression (Fig. S6). Considering the transfection efficiency of C2C12 cells, it is likely that the expanded CUG repeat could alter H-Ras expression. However, involvement of Ras in DM1 has not been reported thus far, and further studies are needed in the future.

DM1 is the most common muscular dystrophy in adults, affecting approximately one in every 8,000 individuals. However, there is as yet no cure for DM. In this study, we showed that manumycin A corrects aberrant splicing of *Clcn1* and revealed that H-Ras is involved in regulation of *Clcn1* splicing. We hope that further studies on manumycin A and H-Ras will lead to a novel therapy for DM1.

Methods

Plasmid construction. Clcn1-L is a luciferase reporter vector containing a genomic segment of mouse *Clcn1* (exon 6 to exon 7) and the firefly luciferase gene. Firefly luciferase (F-Luc) was amplified from the downstream of SV40 promoter of the pGL-3 promoter vector (Promega, Madison, WI, USA) by PCR using *PfuUltra* High-Fidelity DNA polymerase (STRATAGENE, La Jolla, CA, USA), generating a 1.7-kb product with the addition of a restriction site for *Sal*I and *Bam*HI. Therefore, this fragment did not contain SV40 promoter. The following primer pair was used: F-Luc forward, 5′-AAAGTCGACCCATGAAGACGCC-3′; and F-Luc reverse, 5′-CCGGATCCTTACACGGCGATCTT-3′. The fragment was inserted into the *Sal*I-*Bam*HI site of the Clcn1 minigene. The Clcn1 minigene contains PCR-amplified fragments of mouse *Clcn1* (exon 6 to exon 7) and has been described previously[22]. The nucleotide sequences of the DNA inserts and reading frame were confirmed to be correct by sequencing. DM18 and DM480 contain a fragment of the 3′ region of *DMPK* with CTG18 or interrupted CTG480 repeats, respectively, and have been described previously[23].

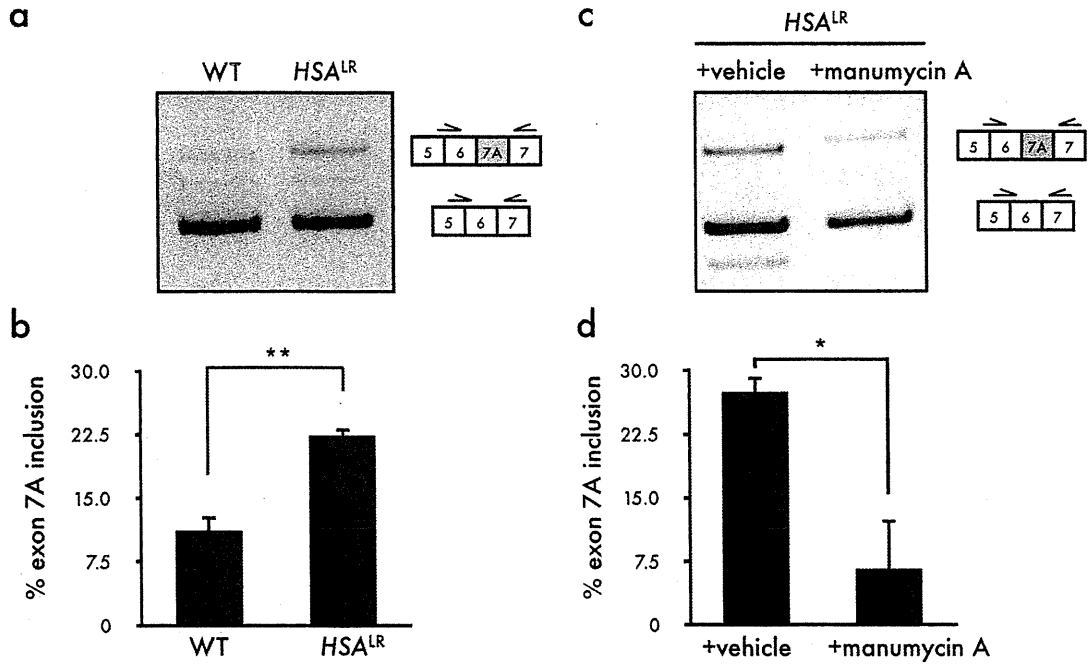

Figure 3 | Manumycin A corrects aberrant splicing of *Clcn1* in HSA^{LR} DM1 model mice. (a) RT-PCR analysis showed increased inclusion of *Clcn1* exon 7A in HSA^{LR} mouse. (b) Quantification of the results shown in (a) (mean + SEM, n = 3). (c) RT-PCR analysis showed reduced inclusion of *Clcn1* exon 7A 5 days after injection of manumycin A into TA muscles. (d) Quantification of the results shown in (a) (Mean + SEM, n = 3). The gel image was cropped around the region of interest and the samples (n = 3) were resolved in the same gel. Statistical significance was determined using *t*-tests ($*p < 0.05$, $**p < 0.01$).

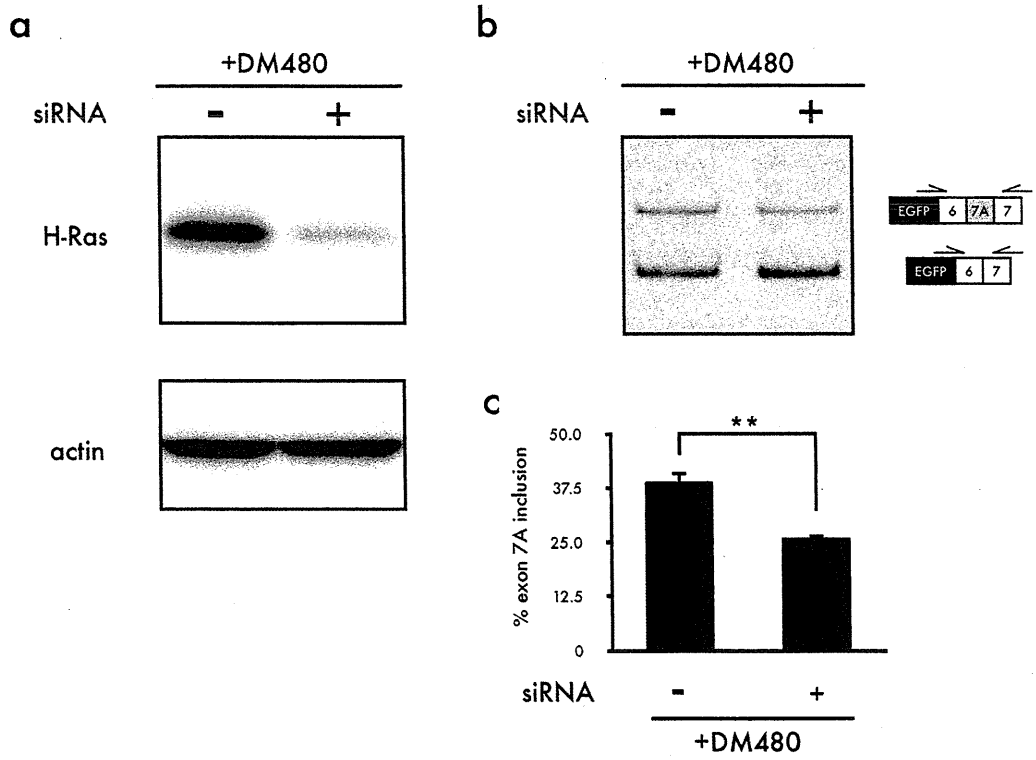

Figure 4 | The knockdown of H-Ras corrects aberrant splicing of *Clcn1* in the presence of the expanded CUG repeat. (a) Representative result of Western blot analysis of H-Ras in C2C12 cells. (b) Results of cellular splicing assays using Clcn1-L minigene, DM480 and siRNA. (c) Quantification of the results shown in (b) (mean + SEM, n = 3). The gel and blot image were cropped around the region of interest and the samples (n = 3) were resolved in the same gel or blot. Statistical significance was determined using *t*-tests ($**p < 0.01$).

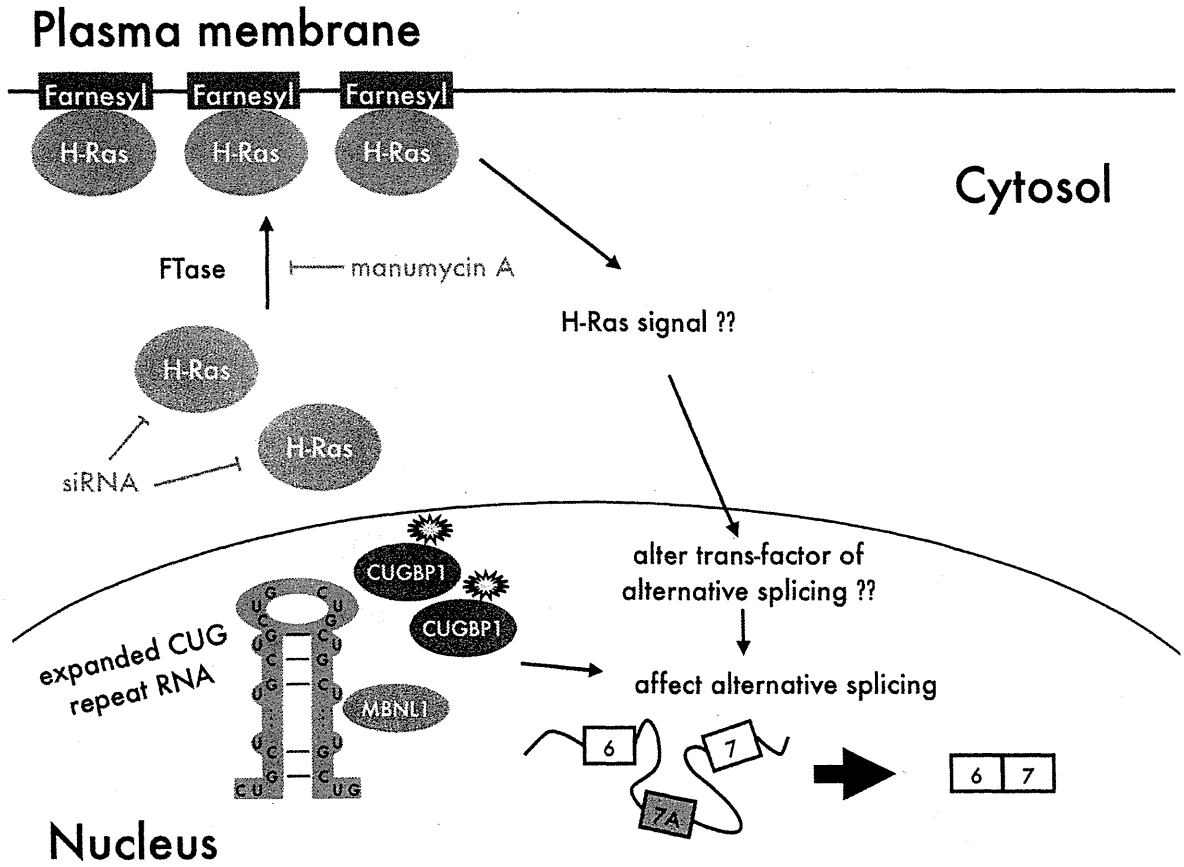

Figure 5 | Model of how manumycin A affects *Clcn1* splicing. In DM1, it is known that expanded CUG repeat RNA transcripts trap MBNL1 and up-regulate CUGBP1, resulting in aberrant regulation of alternative splicing. However, manumycin A does not affect the expression of these proteins. Manumycin A might act as a Ras farnesyltransferase inhibitor, thereby altering H-Ras signaling. This could in turn result in alteration of a *trans*-acting factor involved in alternative splicing other than MBNL1 and CUGBP1.

Cell culture and transfection. C2C12 cells were cultured in Dulbecco's modified Eagle's medium supplemented with 20% (v/v) fetal bovine serum and then incubated at 37°C with 5% CO_2. For the minigene and luciferase reporter assays, C2C12 cells were transfected with plasmids for expression of a minigene with toxic RNA transcripts using Lipofectamine 2000 reagent (Invitrogen, Carlsbad, CA, USA). Transfection was conducted according to the manufacturer's protocol. Cells were cultured in 24- and 96-well plates for the minigene and luciferase reporter assays, respectively.

Luciferase reporter assay and drug screening. Culture, transfection, cell harvesting, and luciferase activity measurements were performed according to the standard methods of the Dual-Glo Luciferase Assay System (Promega). *Clcn1*-L and *DM480* were co-expressed in cells. Plasmid pRL (Promega), which contains the sea pansy luciferase gene, was co-transfected as an internal control for normalization of transfection efficiency. In all experiments, luciferase activity was measured 48 h after transfection and was assayed using the Dual-Glo Luciferase Assay System (Promega). Firefly and sea pansy luciferase activities were measured using the Centro LB 960 (Berthold, Bad Wildbad, Germany), and the value of each sample was calculated as light units of firefly luciferase per light unit of sea pansy. The ICCB Known Bioactives Library (Enzo Life Sciences, Farmingdale, NY, USA) was referenced for drug screening. Chemical compounds were added 24 h after transfection at 0.1% (v/v), and luciferase activity was measured 24 h after the addition of chemical compounds.

Administration of manumycin A to DM mice. HSA^{LR} transgenic mice were used for animal experiments and have been described previously[45]. These mice express human skeletal actin mRNA, with approximately 250 CUG repeats in the 3′-UTR. Manumycin A was diluted to a final concentration of 75 ng/μl in saline containig 0.1% DMSO. Manumycin A (40 μl, 3.0 μg) or vehicle (0.1% DMSO in saline) was injected into the TA muscles of opposite limbs. Mice were killed 5 days after injection, and TA muscle was obtained for splicing analysis. All experiments were conducted according to the Regulations for Animal Experimentation at the University of Tokyo (Tokyo, Japan).

Identification of Clcn1 splice variants. Total RNA was isolated using a GenElute Mammalian Total RNA Miniprep kit (Sigma-Aldrich, St. Louis, MO, USA). cDNA synthesis was performed using a Prime-Script First Strand cDNA Synthesis Kit (TAKARA BIO, Otsu, Japan) with an oligo dT primer. The Clcn1-L minigene fragments were amplified by PCR (24–27 cycles) with the following primer pair: Clcn1-L forward, 5′-CATGGTCCTGCTGGAGTTCGTG-3′; and Clcn-L reverse, 5′-CTCCAAGTGGTGTTCCAAAACAGC-3′. To detect endogenous *Clcn1* fragments, PCR amplification (32-34 cycles) was carried out with the following primer pair: *Clcn1* forward, 5′-GCTGCTGTCCTCAGCAAGTT-3′; and *Clcn1* reverse, 5′-CTGAATGTGGCTGCAAAGAA-3′. PCR products were resolved on 8% polyacrylamide gels and stained with ethidium bromide. Band intensities were quantified using an LAS-3000 instrument and Multigauge software (FUJIFILM, Tokyo, Japan). The ratio of exon 7A inclusion in *Clcn1* was calculated as (7A inclusion)/(7A inclusion + 7A exclusion) × 100.

RNA interference. An siRNA specific for H-Ras (H-Ras siRNA) and a negative control siRNA (MISSION siRNA Universal Negative Control) were purchased from Sigma-Aldrich. The siRNA target sequences were as follows: mouse H-Ras siRNA sense, 5′- GUUGCAUCACAGUAAAUUAdTdT-3′; and mouse H-Ras siRNA antisense, 5′- UAAUUUACUGUGAUGCAACdTdT-3′. The efficacy of the RNAi-mediated knockdown of endogenous H-Ras and actin expression was determined by Western blot analysis. Antibodies specific for H-Ras (C-20; Santa Cruz Biotechnology, Santa Cruz, CA, USA,) and actin (A2066; Sigma-Aldrich) were used.

1. Harper, P. S. *Myotonic Dystophy, third edn.* (2001).
2. Ranum, L. P. & Cooper, T. A. RNA-mediated neuromuscular disorders. *Annu Rev Neurosci* **29**, 259–277 (2006).
3. Aslanidis, C. *et al.* Cloning of the essential myotonic dystrophy region and mapping of the putative defect. *Nature* **355**, (1992).
4. Brook, J. D. *et al.* Molecular basis of myotonic dystrophy: expansion of a trinucleotide (CTG) repeat at the 3' end of a transcript encoding a protein kinase family member. *Cell* **69**, 385 (1992).
5. Liquori, C. L. *et al.* Myotonic dystrophy type 2 caused by a CCTG expansion in intron 1 of ZNF9. *Science* **293**, 864–867 (2001).
6. Machuca-Tzili, L., Brook, D. & Hilton-Jones, D. Clinical and molecular aspects of the myotonic dystrophies: a review. *Muscle Nerve* **32**, 1–18 (2005).

7. Mankodi, A. *et al.* Expanded CUG repeats trigger aberrant splicing of ClC-1 chloride channel pre-mRNA and hyperexcitability of skeletal muscle in myotonic dystrophy. *Mol Cell* **10**, 35–44 (2002).
8. Taneja, K. L., McCurrach, M., Schalling, M., Housman, D. & Singer, R. H. Foci of trinucleotide repeat transcripts in nuclei of myotonic dystrophy cells and tissues. *J Cell Biol* **128**, 995–1002 (1995).
9. Fardaei, M. *et al.* Three proteins, MBNL, MBLL and MBXL, co-localize in vivo with nuclear foci of expanded-repeat transcripts in DM1 and DM2 cells. *Hum Mol Genet* **11**, 805–814 (2002).
10. Kino, Y. *et al.* Muscleblind protein, MBNL1/EXP, binds specifically to CHHG repeats. *Hum Mol Genet* **13**, 495–507 (2004).
11. Miller, J. W. *et al.* Recruitment of human muscleblind proteins to (CUG)(n) expansions associated with myotonic dystrophy. *EMBO J* **19**, 4439–4448 (2000).
12. Timchenko, L. T. *et al.* Identification of a (CUG)n triplet repeat RNA-binding protein and its expression in myotonic dystrophy. *Nucleic Acids Res* **24**, 4407–4414 (1996).
13. Holt, I. *et al.* Muscleblind-like proteins: similarities and differences in normal and myotonic dystrophy muscle. *Am J Pathol* **174**, 216–227 (2009).
14. Kuyumcu-Martinez, N. M., Wang, G. S. & Cooper, T. A. Increased steady-state levels of CUGBP1 in myotonic dystrophy 1 are due to PKC-mediated hyperphosphorylation. *Mol Cell* **28**, 68–78 (2007).
15. Koebis, M. *et al.* Alternative splicing of myomesin 1 gene is aberrantly regulated in myotonic dystrophy type 1. *Genes Cells* **16**, 961–972 (2011).
16. Ohsawa, N., Koebis, M., Suo, S., Nishino, I. & Ishiura, S. Alternative splicing of PDLIM3/ALP, for α-actinin-associated LIM protein 3, is aberrant in persons with myotonic dystrophy. *Biochem Biophys Res Commun* **409**, 64–69 (2011).
17. Gomes-Pereira, M., Cooper, T. A. & Gourdon, G. Myotonic dystrophy mouse models: towards rational therapy development. *Trends Mol Med* **17**, 506–517 (2011).
18. Charlet-B, N. *et al.* Loss of the muscle-specific chloride channel in type 1 myotonic dystrophy due to misregulated alternative splicing. *Mol Cell* **10**, 45–53 (2002).
19. Fugier, C. *et al.* Misregulated alternative splicing of BIN1 is associated with T tubule alterations and muscle weakness in myotonic dystrophy. *Nat Med* **17**, 720–725 (2011).
20. Savkur, R. S., Philips, A. V. & Cooper, T. A. Aberrant regulation of insulin receptor alternative splicing is associated with insulin resistance in myotonic dystrophy. *Nat Genet* **29**, 40–47 (2001).
21. Berg, J., Jiang, H., Thornton, C. A. & Cannon, S. C. Truncated ClC-1 mRNA in myotonic dystrophy exerts a dominant-negative effect on the Cl current. *Neurology* **63**, 2371–2375 (2004).
22. Kino, Y. *et al.* MBNL and CELF proteins regulate alternative splicing of the skeletal muscle chloride channel CLCN1. *Nucleic Acids Res* **37**, 6477–6490 (2009).
23. Kanadia, R. N. *et al.* Reversal of RNA missplicing and myotonia after muscleblind overexpression in a mouse poly(CUG) model for myotonic dystrophy. *Proc Natl Acad Sci U S A* **103**, 11748–11753 (2006).
24. Langlois, M. A. *et al.* Cytoplasmic and nuclear retained DMPK mRNAs are targets for RNA interference in myotonic dystrophy cells. *J Biol Chem* **280**, 16949–16954 (2005).
25. Wheeler, T. M. *et al.* Reversal of RNA dominance by displacement of protein sequestered on triplet repeat RNA. *Science* **325**, 336–339 (2009).
26. Warf, M. B., Nakamori, M., Matthys, C. M., Thornton, C. A. & Berglund, J. A. Pentamidine reverses the splicing defects associated with myotonic dystrophy. *Proc Natl Acad Sci U S A* **106**, 18551–18556 (2009).
27. Lee, J. E., Bennett, C. F. & Cooper, T. A. RNase H-mediated degradation of toxic RNA in myotonic dystrophy type 1. *Proc Natl Acad Sci U S A* **109**, 4221–4226 (2012).
28. Wang, G. S. *et al.* PKC inhibition ameliorates the cardiac phenotype in a mouse model of myotonic dystrophy type 1. *J Clin Invest* **119**, 3797–3806 (2009).
29. Sattler, I., Thiericke, R. & Zeeck, A. The manumycin-group metabolites. *Nat Prod Rep* **15**, 221–240 (1998).
30. Hara, M. *et al.* Identification of Ras farnesyltransferase inhibitors by microbial screening. *Proc Natl Acad Sci U S A* **90**, 2281–2285 (1993).
31. Gelb, M. H. Protein prenylation, et cetera: signal transduction in two dimensions. *Science* **275**, 1750–1751 (1997).
32. Glomset, J. A. & Farnsworth, C. C. Role of protein modification reactions in programming interactions between ras-related GTPases and cell membranes. *Annu Rev Cell Biol* **10**, 181–205 (1994).
33. Mumby, S. M. Reversible palmitoylation of signaling proteins. *Curr Opin Cell Biol* **9**, 148–154 (1997).
34. Scheffzek, K. *et al.* The Ras-RasGAP complex: structural basis for GTPase activation and its loss in oncogenic Ras mutants. *Science* **277**, 333–338 (1997).
35. Fiordalisi, J. J. *et al.* High affinity for farnesyltransferase and alternative prenylation contribute individually to K-Ras4B resistance to farnesyltransferase inhibitors. *J Biol Chem* **278**, 41718–41727 (2003).
36. Kimura, T. *et al.* Altered mRNA splicing of the skeletal muscle ryanodine receptor and sarcoplasmic/endoplasmic reticulum Ca2+-ATPase in myotonic dystrophy type 1. *Hum Mol Genet* **14**, 2189–2200 (2005).
37. Lin, X. *et al.* Failure of MBNL1-dependent post-natal splicing transitions in myotonic dystrophy. *Hum Mol Genet* **15**, 2087–2097 (2006).
38. Hino, S. *et al.* Molecular mechanisms responsible for aberrant splicing of SERCA1 in myotonic dystrophy type 1. *Hum Mol Genet* **16**, 2834–2843 (2007).
39. Ward, A. J., Rimer, M., Killian, J. M., Dowling, J. J. & Cooper, T. A. CUGBP1 overexpression in mouse skeletal muscle reproduces features of myotonic dystrophy type 1. *Hum Mol Genet* **19**, 3614–3622 (2010).
40. Olson, M. F. & Marais, R. Ras protein signalling. *Semin Immunol* **12**, 63–73 (2000).
41. Blaustein, M., Pelisch, F. & Srebrow, A. Signals, pathways and splicing regulation. *Int J Biochem Cell Biol* **39**, 2031–2048 (2007).
42. Blaustein, M. *et al.* Concerted regulation of nuclear and cytoplasmic activities of SR proteins by AKT. *Nat Struct Mol Biol* **12**, 1037–1044 (2005).
43. Weg-Remers, S., Ponta, H., Herrlich, P. & König, H. Regulation of alternative pre-mRNA splicing by the ERK MAP-kinase pathway. *EMBO J* **20**, 4194–4203 (2001).
44. Lee, J. *et al.* Proto-oncogenic H-Ras, K-Ras, and N-Ras are involved in muscle differentiation via phosphatidylinositol 3-kinase. *Cell Res* **20**, 919–934 (2010).
45. Mankodi, A. *et al.* Myotonic dystrophy in transgenic mice expressing an expanded CUG repeat. *Science* **289**, 1769–1773 (2000).

Acknowledgements

We thank Prof. Charles A. Thornton (University of Rochester) for providing us *HSA*^{LR} mice. We also thank Dr. Yoshihiro Kino for providing us the Clcn1 minigenes, DM18 and DM480 constructs. This work was supported by an intramural research grants (23–5) for Neurological and Psychiatric Disorders of NCNP from the Ministry of Health, Labour and Welfare, Japan, and by the Uesugi Foundation.

Author contributions

K.O., Y.O. and S.I. designed the experiments; K.O. performed all experiments; Y.O. assisted with the construction of the reporter vector; S.S. assisted with the interpretation of the results; M.P.T. prepared the mice; S.T. prepared the small chemical compound library; N.I. supported the project; S.I. supervised the work; and K.O. analyzed the data and wrote the manuscript.

Additional information

Supplementary information accompanies this paper at http://www.nature.com/scientificreports

Competing financial interests: The authors declare no competing financial interests.

How to cite this article: Oana, K. *et al.* Manumycin A corrects aberrant splicing of *Clcn1* in myotonic dystrophy type 1 (DM1) mice. *Sci. Rep.* 3, 2142; DOI:10.1038/srep02142 (2013).

SCIENTIFIC REPORTS

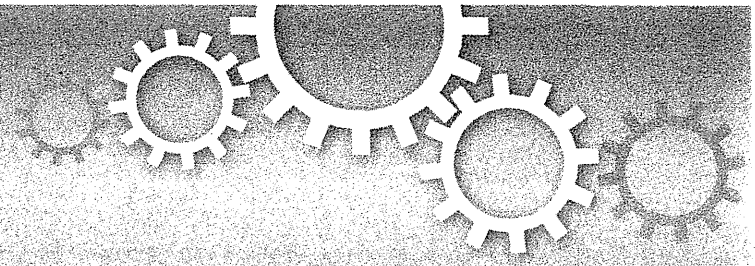

OPEN

SUBJECT AREAS:
MECHANISMS OF DISEASE
ANTISENSE OLIGO
DRUG DELIVERY
RNA SPLICING

Received
18 March 2013

Accepted
21 June 2013

Published
22 July 2013

Correspondence and requests for materials should be addressed to S.I. (cishiura@mail.ecc.u-tokyo.ac.jp)

Ultrasound-enhanced delivery of Morpholino with Bubble liposomes ameliorates the myotonia of myotonic dystrophy model mice

Michinori Koebis[1], Tamami Kiyatake[1], Hiroshi Yamaura[1], Kanako Nagano[1], Mana Higashihara[2], Masahiro Sonoo[3], Yukiko Hayashi[4], Yoichi Negishi[5], Yoko Endo-Takahashi[5], Dai Yanagihara[1], Ryoichi Matsuda[1], Masanori P. Takahashi[6], Ichizo Nishino[4] & Shoichi Ishiura[1]

[1]Graduate School of Arts and Sciences, the University of Tokyo, Tokyo, Japan, [2]Division of Neurology, Department of Internal Medicine 3, National Defense Medical College, Saitama, Japan, [3]Department of Neurology, Teikyo University School of Medicine, Tokyo, Japan, [4]Department of Neuromuscular Research, National Institute of Neuroscience, National Center of Neurology and Psychiatry (NCNP), Tokyo, Japan, [5]Department of Drug Delivery and Molecular Biopharmaceutics, School of Pharmacy, Tokyo University of Pharmacy and Life Sciences, Tokyo, Japan, [6]Department of Neurology, Osaka University Graduate School of Medicine, Osaka, Japan.

Phosphorodiamidate morpholino oligonucleotide (PMO)-mediated control of the alternative splicing of the chloride channel 1 (*CLCN1*) gene is a promising treatment for myotonic dystrophy type 1 (DM1) because the abnormal splicing of this gene causes myotonia in patients with DM1. In this study, we optimised a PMO sequence to correct *Clcn1* alternative splicing and successfully remedied the myotonic phenotype of a DM1 mouse model, the HSA^{LR} mouse. To enhance the efficiency of delivery of PMO into HSA^{LR} mouse muscles, Bubble liposomes, which have been used as a gene delivery tool, were applied with ultrasound exposure. Effective delivery of PMO led to increased expression of Clcn1 protein in skeletal muscle and the amelioration of myotonia. Thus, PMO-mediated control of the alternative splicing of the *Clcn1* gene must be important target of antisense therapy of DM1.

Myotonic dystrophy type 1 (DM1) is caused by expansion of the CTG repeat in the 3′ untranslated region (UTR) of the *DMPK* gene[1–4]. Patients with DM1 show multi-systemic symptoms, including muscle wasting, muscle weakness, myotonia, cardiac conduction defect, cataracts, mental retardation and insulin resistance[5]. A patient, however, does not always present with all of these symptoms and the severity of the disease varies among individuals. Among the symptoms, myotonia is the most prominent and common phenotype of DM1: most patients feel muscle stiffness and difficulty in relaxing muscles soon after developing the disease.

The characteristic feature of the pathology of DM1 is the aberrant regulation of dozens of alternative splicing events, and some of the abnormal splicing events have been suggested to be involved in some of the symptoms[6–10]. Myotonic discharge is thought to be caused by the aberrant alternative splicing of the chloride channel 1 (*CLCN1*) gene[11,12]. In patients with DM1, extra exons from intron 6 are spliced into the *CLCN1* mRNA, leading to the appearance of a premature termination codon in the subsequent exon, degradation of the mRNA by nonsense-mediated decay and decreased expression of CLCN1 protein[11]. The idea that abnormal splicing of the *CLCN1* gene causes myotonia is strongly supported by the fact that the *CLCN1* gene is the only gene responsible for congenital myotonia, and the identification of multiple mutations in patients with the disease and their families[13]. Wheeler and his colleagues corrected the abnormal splicing of the *Clcn1* gene in a DM1 mouse model, the HSA^{LR} mouse, by using an antisense oligonucleotide (AON) and successfully alleviated the myotonic phenotype[14]. Thus, correction of the abnormally regulated splicing is a promising treatment for DM1.

An AON is a short, synthetic nucleic acid molecule with a sequence complementary to a target transcript. It can be used to manipulate an alternative splicing event: the AON that binds to the region around the target exon, specifically splice sites or splicing enhancer domains, physically blocks assembly of the spliceosome on the exon and induces exon skipping[15]. The efficacy of an AON is dependent on its half-life, affinity for its target RNA and *in*

vivo kinetics. A variety of AON molecules with 2′-*O* modifications and/or unnatural backbones have been developed to improve nuclease resistance and affinity for RNA[15]. Among them, Morpholino (also referred as phosphorodiamidate morpholino oligonucleotide [PMO]) is one of the most hopeful AONs. PMO has morpholine rings linked with phosphorodiamidate linkages in its backbone instead of deoxyribose and phosphodiester bonds. Due to its completely unnatural chemistry, PMO is hardly recognised by cellular nucleases. It has higher affinity for RNA than for DNA; the T_m value of a hybrid of PMO and RNA is much higher than that of DNA and RNA[16]. Several papers have reported the local and systemic administration of PMO to mice and dogs. For example, when a high dose of PMO (3 g/kg) was administrated intravenously into the *mdx* mouse, a mouse model of Duchenne muscular dystrophy, the PMO entered skeletal muscle without any assistive delivery reagent[17]. However, unlike mdx mice, muscle penetration of Evans Blue dye did not increase in HSA^{LR} and wild-type mice[18], which indicated a physical barrier to PMO uptake should be grater in HSA^{LR} than in *mdx*. In preceding reports on PMO treatment in HSA^{LR}, intravenous administration of CAG25 PMO led no detectable improvements in *Serca1* splicing in HSA^{LR} mice[19], and even when PMO was injected intramuscularly its uptake was limited to the needle track[14]. In these studies, they used electroporation to administer unmodified PMO intramuscularly, so we investigated a less invasive PMO delivery method to develop PMO treatment for DM1.

Recently, ultrasound exposure has been used for the intracellular delivery of molecules such as dextran, plasmid DNA and siRNA. If ultrasound is sufficiently strong, it will generate microscopic vacuum bubbles in a solution by a process known as inertial cavitation. The bubbles immediately collapse, producing a shock wave, which is believed to transiently increase the permeability of cell membranes in the vicinity. Inertial cavitation is enhanced by using micro bubbles of echo-contrast gas. This method has been applied to gene delivery into various mouse tissues, including skeletal muscle, liver and tumour tissues[20–22]; however, introducing genes into deep tissues with microbubbles is difficult because of their size and instability. To overcome these problems, we previously developed a novel drug delivery reagent coined "Bubble liposomes", polyethylene glycol-modified liposomes (PEG liposomes) encapsulating echo-contrast gas[23]. Owing to the stability in serum and uniform microscopic size of PEG liposomes, we successfully delivered genes and siRNA into several tissues[24–28]. However, does the Bubble liposome-ultrasound delivery system efficiently deliver PMO into skeletal muscles in the HSA^{LR} mice? In this study, we examined the ability of the Bubble liposome-ultrasound system to deliver PMO into skeletal muscles of HSA^{LR} mice as a treatment for abnormal splicing.

We newly designed antisense PMOs targeting exon 7A of the *Clcn1* gene and delivered them into HSA^{LR} mice. The PMOs were successfully delivered into skeletal muscles by the Bubble liposome-ultrasound system, which decreased the inclusion of exon 7A *in vivo*. Furthermore, the injection of PMO ameliorated the myotonic phenotype of the model mice. Our results suggest that Bubble liposomes should be effective for delivering PMOs into muscle tissues and can be applied to PMO treatment of DM1.

Results

We first determined the optimal target sequence of the *Clcn1* pre-mRNA to promote skipping of exon 7A. To achieve this, we used a *Clcn1* minigene and examined its alternative splicing using a cell culture-based assay. The minigene contains the genomic region from exon 6 to exon 7 of the murine *Clcn1* gene. When it was transfected into COS-7 cells, approximately 50% of transcripts contained exon 7A (Fig. 1b, minigene only). To screen for an optimal AON sequence, we used 25-mer phosphorothioate 2′ *O*-methyl (PS2OMe) RNA, which can regulate alternative splicing by sterically preventing spliceosomal assembly, just like PMO. We examined PS2OMe RNA molecules that covered the whole of exon 7A (1–25, 26–50, 51–75 and 76–90) and the boundary of intron 6 and exon 7A (−10–15). We transfected the minigene together with the PS2OMe RNA into COS-7 cells and analysed the alternative splicing of the minigene. We found that −10–15 and 1–25 PS2OMe significantly reduced the rate of inclusion of exon 7A, with 1–25 PS2OMe being the most effective molecule (Fig. 1b).

Previously, we identified the 8 nt at the 5′ end of exon 7A as an exonic splicing enhancer (ESE) essential for basal inclusion of the exon[29]. Given that both −10–15 and 1–25 PS2OMe covered the ESE, and that 1–25 PS2OMe seemed to be more effective at excluding exon 7A, we speculated that another ESE (16–25) would be located in the region +16 to +25, and that 1–25 PS2OMe would not share it with −10–15 PS2OMe. To examine this possibility, we tested whether 16–40 PS2OMe enhanced normal splicing. 16–40 PS2OMe markedly reduced the rate of inclusion of exon 7A of the *Clcn1* minigene (Supplementary Fig. S1). As 26–50 PS2OMe did not change the alternative splicing, we conclude that the other ESE (16–25) is important for exon 7A inclusion. Thus, we used 1–25 AON, which targeted both ESEs, in subsequent experiments.

PS2OMe is highly resistant to nuclease-mediated degradation owing to its phosphorothioate linkages; however, it is still degraded slowly and releases monomers that have a toxic, free phosphorothioate group. In contrast, PMO is remarkably resistant to degradation and is not noxious. Therefore, we next investigated whether a PMO with the same sequence as 1–25 PS2OMe also improved the alternative splicing of exon 7A by using the cell culture-based splicing assay (Fig. 1c). The −11–14 PMO we used here had the same sequence as that Wheeler and his colleagues used in a previous study[14]. RT-PCR analysis showed that both 1–25 and −11–14 PMOs significantly reduced exon 7A inclusion. Although the effect of 1–25 PMO was greater than that of −11–14 PMO, no statistically significant difference was observed between them.

1–25 PMO was so effective at improving alternative splicing of the *Clcn1* minigene in cultured cells that we expected it to work well *in vivo*. To test whether 1–25 PMO could work *in vivo*, we administrated 60 μg of 1–25 PMO intramuscularly four times at weekly intervals into the *tibialis anterior* (TA) muscles of HSA^{LR} mice. The alternative splicing of the *Clcn1* gene was moderately improved, with an approximately 30% decrease in exon 7A inclusion. Electromyography (EMG) with a single needle electrode, however, revealed that the occurrence of myotonia was not altered by PMO injection (Supplementary Fig. S2). Because 60 μg of PMO was quite a high dose for administration into a single muscle, we assumed that an effective delivery system would be required to introduce 1–25 PMO into muscle tissues. We therefore examined the usefulness of ultrasound-enhanced delivery with Bubble liposomes for PMO delivery. We administrated 20 μg of 1–25 PMO three times at weekly intervals into the TA muscles of HSA^{LR} mice with or without Bubble liposomes and ultrasound (Fig. 2). RT-PCR analysis revealed that the rate of inclusion of exon 7A decreased to its lowest level when both Bubble liposomes and ultrasound were applied, indicating that use of the combination of Bubble liposomes and ultrasound could enhance PMO delivery efficiency.

We next investigated whether 1–25 PMO could cure myotonic symptoms in HSA^{LR} mice when delivered using the Bubble liposome-ultrasound system. We administrated 1–25 PMO as described above. Three weeks later, we harvested the injected muscles and conducted RT-PCR and immunohistological analyses. RT-PCR showed that 1–25 PMO decreased the inclusion of exon 7A to a level comparable to that in wild-type FVB/n mice (Fig. 3a). We checked four other alternative splicing events, *Cypher* (*Ldb3*) exon 11, *Mbnl1* exon 5, *Ryr1* exon 70 and *Serca1* exon 22, which are known to be abnormally regulated in patients with DM1and HSA^{LR} mice[30]. We found that the alternative splicing of none of them was changed by

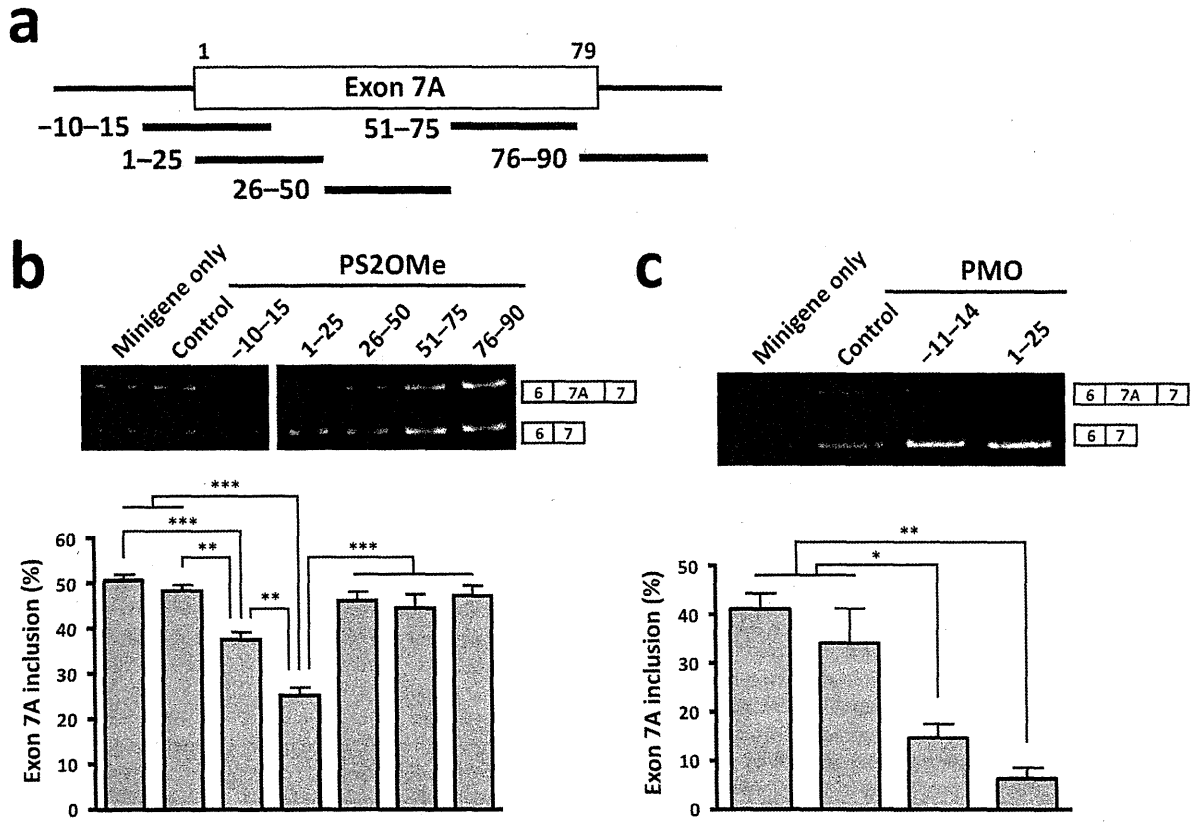

Figure 1 | AON-mediated exclusion of *Clcn1* exon 7A in COS-7 cells. (a) Locations of the target sites of AONs (thick black lines) along the *Clcn1* pre-mRNA. The numbers over exon 7A (rectangle) indicate the positions of nucleotides. (b) Cellular splicing assay to detect the exclusion of exon 7A of the *Clcn1* minigene by PS2OMe RNA in COS-7 cells. 1–25 was the most successful AON. A representative result is shown above and the bars indicate mean and s.e.m. ($n = 6$). (c) The same assay as in (b) except that PMOs were used. 1–25 PMO decreased the inclusion of exon 7A effectively ($n = 3$). Statistical significance was analysed by Tukey's multi-comparison test (* $P < 0.05$, ** $P < 0.01$, *** $P < 0.001$).

the injection of 1–25 PMO (Fig. 3b); thus, the effect of the PMO was specific to the alternative splicing of the *Clcn1* gene.

The abnormal splicing of *Clcn1* is believed to cause myotonia by introducing a premature termination codon into the subsequent exon and by decreasing the expression of the Clcn1 protein via nonsense-mediated mRNA decay. Thus, we examined whether 1–25 PMO restored the expression of Clcn1 protein in HSA^{LR} mice. Immunofluorescence analysis of TA muscles showed the sarcolemmal localisation of Clcn1 protein in wild-type muscle, but such a pattern was not detected in saline-injected HSA^{LR} mice. The injection of 1–25 PMO clearly restored the sarcolemmal distribution, demonstrating that correction of the abnormal splicing of the *Clcn1* gene led to the normal expression of its protein (Fig. 3c).

Finally, we investigated whether injection of 1–25 PMO improved the myotonic phenotype of HSA^{LR} mice. Electromyographic analyses showed bursts of action potentials after electrical stimulation (4–8 V) in HSA^{LR} mice, but not in wild-type mice (Fig. 4a). Myotonia occurred even in denervated muscles (data not shown), which indicates that it was not caused by hyperactivation of motor neurones, but by increased excitability of the sarcolemma. Myotonic EMG activities continued for 1 to 3 s and their average duration was 1.27 s in saline-treated TA muscles. The injection of 1–25 PMO decreased their duration, but the change was not statistically significant; the integrated EMG (iEMG) was reduced by the PMO administration ($P < 0.05$). The decreased iEMG indicated that 1–25 PMO mitigated the hyperexcitability of the HSA^{LR} muscles.

These results suggest that 1–25 PMO could improve the function of the *Clcn1* gene in the DM1 model mouse at the RNA, protein and

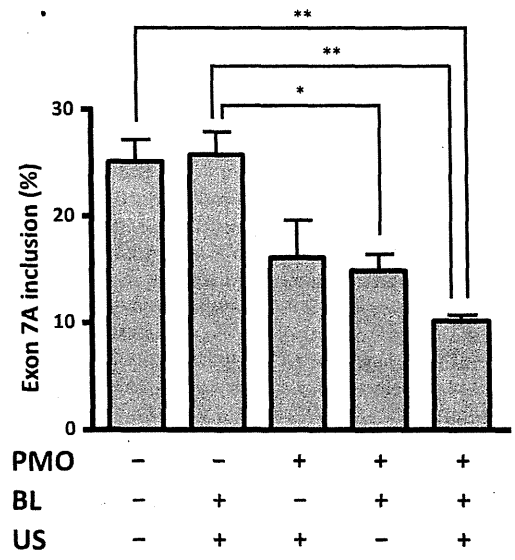

Figure 2 | PMO delivery by the combination of Bubble liposomes and ultrasound. 1–25 PMO (20 μg) or saline was locally administrated into TA muscles of HSA^{LR} mice with/without Bubble liposomes (BLs) and ultrasound (US). The inclusion rate of exon 7A decreased most when both Bubble liposomes and ultrasound were applied. ($n = 3$). The bars indicate mean and s.e.m., and statistical significance was analysed by Tukey's multi-comparison test (* $P < 0.05$, ** $P < 0.01$).

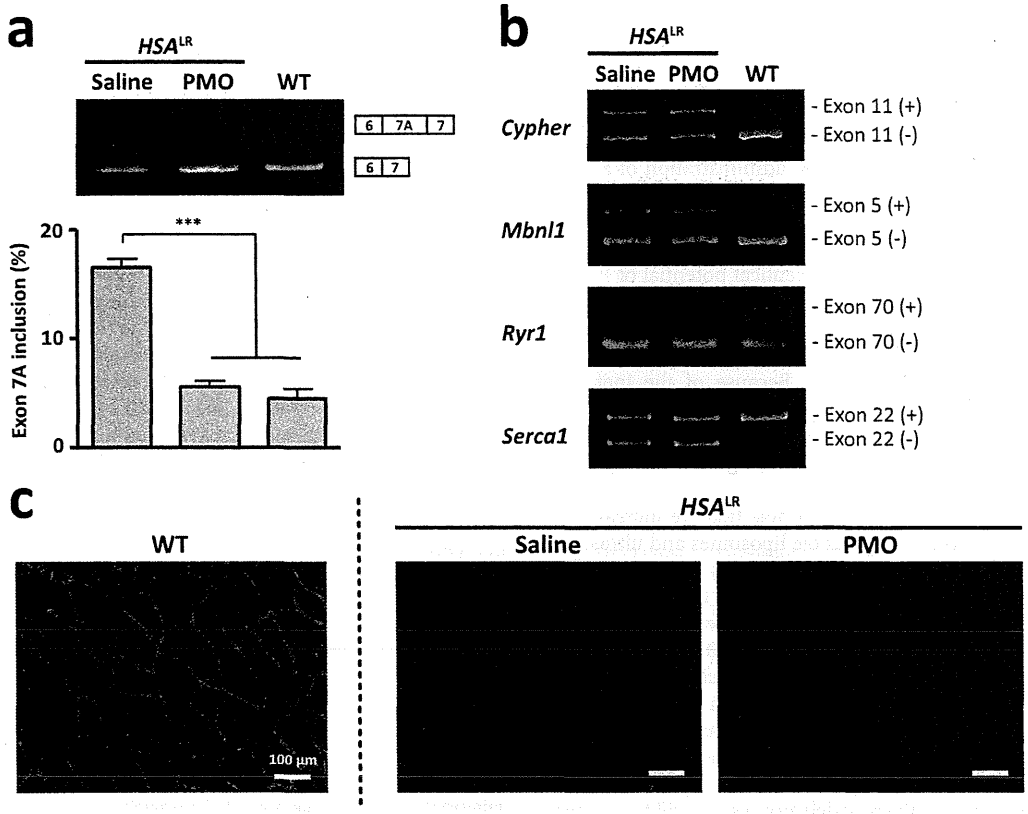

Figure 3 | *In vivo* improvement of aberrant splicing of the *Clcn1* gene by 1–25 PMO. (a) The alternative splicing of *Clcn1* exon 7A in HSA^{LR} and WT mice. 1–25 PMO (20 μg) or saline was locally administrated into TA muscles of HSA^{LR} mice. The ratio of the splicing variant containing exon 7A in thevPMO-injected muscles decreased to a level comparable with that in WT muscle ($n = 5$). The bars indicate mean and s.e.m., and statistical significance was analysed by Tukey's multi-comparison test (*** $P < 0.001$). (b) Abnormal splicing of other genes in HSA^{LR} mice was not affected by 1–25 PMO. (c) Immunofluorescence analysis of transverse sections of TA muscle with an anti-Clcn1 antibody. Injection of 1–25 PMO restored the sarcolemmal localisation of Clcn1 protein in TA muscles of HSA^{LR} mice.

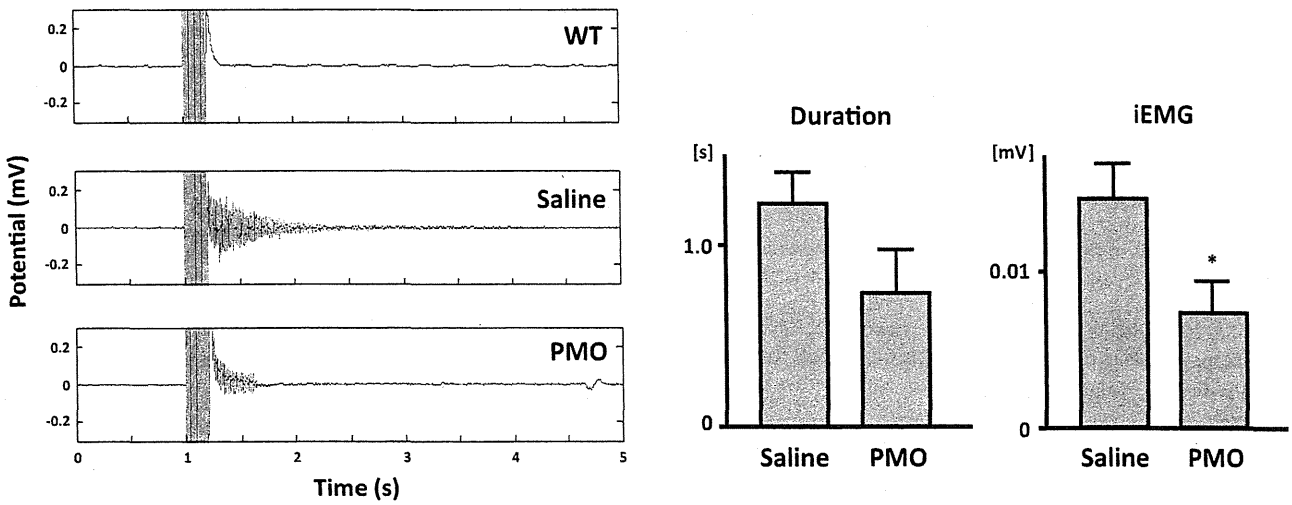

Figure 4 | Reduction of myotonic discharge by 1–25 PMO in HSA^{LR} mice. (a) Representative EMG signals of TA muscle. Tibialis muscle was electrically stimulated 1 s after the EMG recording started. In the HSA^{LR} muscle, repetitive discharges that were absent in the WT muscle could be seen. (b)vDuration of myotonic discharge and integrated EMG (iEMG). 1–25 PMO significantly reduced iEMG in HSA^{LR} muscle (saline, $n = 6$; 1–25 PMO, $n = 7$).The bars indicate mean and s.d., and statistical significance was analysed by Student's *t*-test (* $P < 0.05$).

phenotypic levels, and that the Bubble liposome-ultrasound system should be capable of delivering enough PMO to ameliorate myotonia.

Discussion

The greatest advantage of PMO is its remarkable innocuity. According to a report from Gene Tools, administration of a single 700 mg/kg dose of PMO to a mouse did not cause any obvious acute toxicity[31], while the 50% lethal dose of phosphorothioate DNA, a first-generation antisense oligonucleotide, was estimated to be 750 mg/kg in mice[32]. The high pharmaceutical potential of PMO is also supported by the fact that safety issues were not raised following its administration to mice and humans; however, PMO must overcome the low permeability of the cell membranes to achieve a significant effect on alternative splicing. Because of the inefficient cellular uptake of PMO, systemic delivery and functional splicing modification were not successful in a mouse model[33]. Therefore, for the clinical application of PMO, establishing an effective delivery method is essential.

The major achievement in this study was that we increased the efficiency of PMO delivery using Bubble liposomes and ultrasound. The use of the ultrasound-mediated delivery system with Bubble liposomes improved the alternative splicing of the *Clcn1* gene in HSA^{LR} mice to a level comparable to that of wild-type mice and decreased myotonic discharges, indicating that the delivery system increased introduction of 1–25 PMO into skeletal muscle. Our results show that the intramuscular injection itself delivered the PMO into muscle to some extent, and so the intramuscular injection might have contributed to the relief of the pathology. However, the Bubble liposome- and ultrasound-mediated enhancement of delivery efficiency suggests that the new delivery system will have a beneficial effect over much less invasive injection, such as intravenous injection, which cannot by itself be expected to promote the entry of PMO into skeletal muscle[19].

A fair amount of the *Clcn1* splicing variant without exon 7A was expressed even in the HSA^{LR} mouse. Because the myotonic discharge of a HSA^{LR} mouse was remedied by correcting *Clcn1* alternative splicing in a previous study[14], abnormal splicing of the gene must be the primary cause of myotonia. The expression levels of the "normal" splicing variant in saline-injected muscles were 57% of that in the wild-type muscles. PMO injection increased the expression about 1.4-fold to 78% of that in wild-type mice. As *Clcn1* heterozygous mutant mice did not show a myotonic phenotype[34], the myotonia in HSA^{LR} mice was unlikely to have been caused by haploinsufficiency of full-length Clcn1 protein. Instead, the truncated protein translated from the exon 7A-countaining mRNA may have dominant-negative activity, since full-length Clcn1 protein functions in a dimeric form. Berg *et al.* showed that the truncated Clcn1 protein did not function as a chloride channel, but rather disturbed the channel activity of full-length Clcn1 protein[35]. In this study, expression of the splicing variant containing exon 7A was decreased by 40% in the PMO-administered group. Thus, this may have contributed to the improvement of the pathology, as well as the increased expression of the exon 7A skipping variant. The dominant-negative hypothesis suggests that the AON therapy should completely prevent exon 7A inclusion when used to treat myotonia, in contrast to Duchenne muscular dystrophy, in which the partial restoration of dystrophin expression could lead to the improvement of muscle strength.

In the course of our search for the optimal PMO sequence to correct *Clcn1* splicing, we found that 1–25 and 16–40 PMOs suppressed the inclusion of exon 7A well, but that 26–50 PMO did not. The fact that steric blocking of the 16–25 region promoted exon skipping indicates that proteins that bind to this region are essential for exon 7A recognition. Previously, we showed that the 8 nt at the 5′ end of exon 7A serve as an ESE and that an RNA-binding protein, Mbnl1, prevented the inclusion of exon 7A by binding to the ESE[29]. Unlike the ESE, the sequence of the 16–25 region was pyrimidine-rich and did not contain the Mbnl1-recognition motif, YGCY. It remains to be determined which proteins bind to the region to regulate exon 7A splicing.

In this study, we tried to cure DM1 model mice using a PMO targeted to *Clcn1*. However, considering that dozens of genes are abnormally spliced in patients with DM1, it might be impractical to treat all symptoms due to mis-splicing of such genes with AONs at the same time. DM1 is caused by expansion of the CTG repeats in the 3′ UTR region of the DMPK gene. Transcripts with these expanded repeats sequester Mbnl proteins, which regulate alternative splicing, leading to global alternative splicing dysfunction[36]. Thus, expanded CUG repeat-containing RNA must be the most important target of antisense therapy for DM1, and many groups have studied the use of CAG repeat-containing AONs to dissociate Mbnl1 proteins from CUG repeat-containing RNA. Some trials to treat DM1 model mice with CAG AONs were successful[19,37], but here again the obstacle to clinical application of the AONs was the lack of an efficient delivery method. Our ultrasound-mediated delivery system with Bubble liposomes must have a beneficial effect on the delivery of CAG-containing AONs.

Methods

AONs. *Phosphorothioate 2′ O-methyl RNA oligonucleotides* and phosphorodiamidate morpholino oligonucleotides were purchased from IDT (Coralville, IA, USA) and Gene Tools (Philomath, OR, USA), respectively. The sequences of the oligonucleotides are listed in Supplementary Table ST1. Both AONs were dissolved in water.

Construct. The *Clcn1* minigene has been described previously[29]. Briefly, a *Clcn1* minigene fragment covering exons 6 to 7 was amplified from mouse genomic DNA by PCR and inserted into the *BglII-SalI* sites of pEGFP-C1 (Clontech Laboratories, Mountain View, CA, USA).

Cellular splicing assay. COS-7 cells were cultured in Dulbecco's modified Eagle's medium (DMEM; Sigma-Aldrich, St. Louis, MO, USA) supplemented with 10% heat-inactivated fetal bovine serum (Life Technologies, Foster City, CA, USA) in a humidified atmosphere containing 5% CO_2 at 37°C.

For the splicing assay, COS-7 cells were cultured in 12-well plates and transfected with 0.1 μg of the *Clcn1* minigene and AONs (0.1 μmol) at 60–80% confluence. Polyethylenimine and Endo-Porter (Gene Tools) were used for the transfection of PS2OMe RNA and PMOs, respectively. Forty-eight hours later, total RNA was extracted from the transfected cells using a GenElute Mammalian Total RNA Miniprep Kit (Sigma-Aldrich).

Animals. HSA^{LR} mice are FVB/n-background transgenic mice that express expanded CTG repeats under the control of the human skeletal actin promoter in skeletal muscle[38]. Compared with the first established line, the number of the repeat was reduced: the mice used in this study carried 180–200 repeats. All the mutant mice showed persistent contraction of gluteal muscles after they bucked. We used FVB/nJcl mice (Clea Japan, Tokyo, Japan) as wild-type controls.

The present study was approved by the Ethical Committee for Animal Experiments at the University of Tokyo, and was carried out in accordance with the Guidelines for Research with Experimental Animals of the University of Tokyo and the NIH Guide for the Care and Use of Laboratory Animals (NIH Guide, revised 1996).

Bubble liposomes. Bubble liposomes were prepared by previously described methods[24]. Briefly, PEG liposomes composed of 1,2-dipalmitoyl-sn-glycero-3-phosphocholine (DPPC) (NOF Corporation, Tokyo, Japan) and 1,2-distearoyl-sn-glycero-3-phosphatidyl-ethanolamine-polyethyleneglycol (DSPE-PEG2000-OMe) (NOF Corporation) at a molar ratio of 94 : 6 were prepared by a reverse phase evaporation method. Briefly, all reagents were dissolved in 1 : 1 (v/v) chloroform/diisopropyl ether. Phosphate-buffered saline was added to the lipid solution, and the mixture was sonicated and then evaporated at 47°C. The organic solvent was completely removed, and the size of the liposomes was adjusted to less than 200 nm using extruding equipment and a sizing filter (pore size: 200 nm) (Nuclepore Track-Etch Membrane; Whatman Plc, Maidstone, Kent, UK). The lipid concentration was measured using a Phospholipid C test (Wako Pure Chemical Industries, Ltd, Osaka, Japan). Bubble liposomes were prepared from liposomes and perfluoropropane gas (Takachio Chemical Ind. Co. Ltd, Tokyo, Japan). First, 2-ml sterilised vials containing 0.8 ml of liposome suspension (lipid concentration: 1 mg/ml) were filled with perfluoropropane gas, capped and then pressurised with a further 3 ml of perfluoropropane gas. The vial was placed in a bath-type sonicator (38 kHz, 250 W) (SONO-CLEANER CA-4481L; Kaijo Denki, Tokyo, Japan) for 1 min to form Bubble liposomes.

Injection of morpholino oligonucleotides with Bubble liposomes and ultrasound. PMO (20 μg) and the Bubble liposome suspension (30 μl) were injected into the TA muscles of HSA^{LR} mice (6 weeks old) using a 30-gauge needle (NIPRO Co., Osaka, Japan). Immediately after injection, ultrasound (frequency, 1 MHz; duty, 50%; intensity, 2.0 W/cm^2; time, 60 s) was applied transdermally downstream of the injection site using a 6-mm diameter probe. A SONITRON 1000 device (Rich-Mar, Chattanooga, TN, USA) was used to generate the ultrasound. We administrated the PMO three times at weekly intervals. Three weeks after the last administration, we performed EMG measurements and then killed the mice and harvested the TA muscles for RT-PCR analysis and immunohistochemistry.

Electromyographic recording and electrical stimulation. Implantation of EMG electrodes and stimulating electrodes was carried out under aseptic conditions on mice anaesthetised with 2% vapourised isoflurane in air. Body temperature was measured rectally and was maintained at 37–38°C using a homeothermic heating pad (BioResearch Center, Aichi, Japan). Bipolar wire electrodes (tip distance, 1–2 mm) made of Teflon-insulated stainless steel wire (76 μm diameter bare, 140 μm coated; cat. no. 791000; A-M Systems, Carlsborg, WA, USA) were implanted in the TA and gastrocnemius (GA) muscles to record EMG activity. The electrical stimulation of the TA muscle was achieved using two wire electrodes that were inserted under the skin over the TA muscle and placed along the longitudinal axis of the muscle. After full recovery from the anaesthesia, alert mice were restrained in a cylindrical mouse-sized cage, with their hind limbs out of the cage to maintain their muscles at their resting lengths. The EMG signals were amplified and bandpass filtered (15 Hz–1 KHz; AB-611J; Nihon-Koden, Co., Tokyo, Japan), digitised with an analog-digital converter (PowerLab 16/30, ADInstruments Ltd, Oxford, UK) and recorded (sampling rate 10 kHz) on a computer. Electrical stimulation consisted of repetitive square pulses (train of 20 pulses at 100 Hz, 1 ms duration) delivered by an isolation unit (SS-202J; Nihon-Koden) connected to a pulse generator (SEN-3401, Nihon-Koden). The stimulus intensity was adjusted to evoke ankle dorsiflexion and avoid overt movements and animal discomfort. EMG measurements were recorded in single-blinded manner.

EMG data analysis. Myotonic EMG activities were easily confirmed by visual inspection and analysed using custom-written MATLAB software (MathWorks, Inc., Natick, MA, USA). EMG signals were full-wave-rectified and filtered with a 20 Hz low-pass second-order Butterworth filter. Offset of the EMG signal was defined as a deflection below three standard deviations from baseline. The baseline level was defined as the mean EMG signal in the resting state before stimulation. Duration of myotonic activities was defined as the period from the termination of stimulation to the offset time. Myotonic activities were integrated during the duration of myotonia and calculated by subtracting the baseline level. To quantify EMG activities per unit time, iEMG values were then calculated as the integrated myotonia value divided by corresponding net duration. The EMG data were analysed in a single-blinded manner.

RT-PCR analysis. Total RNA was extracted from TA muscles and cultured cells using TRIzol reagent (Life Technologies) and a GenElute Mammalian Total RNA Miniprep Kit (Sigma-Aldrich), respectively, according to the manufacturers' instructions.

Typically, 0.5–1.0 μg of total RNA was reverse-transcribed with a PrimeScript 1st Strand cDNA Synthesis Kit (Takara Bio, Shiga, Japan) using oligo(dT) primers. PCR reactions were performed using Ex Taq DNA polymerase (Takara Bio). The sequences of the PCR primers are listed in Supplementary Table ST2. The products were electrophoretically resolved on an 8% polyacrylamide gel that was stained with ethidium bromide and analysed using an LAS-3000 luminescence image analyser (FujiFilm, Tokyo, Japan). The ratio of exon 7A inclusion in *Clcn1* mRNA was calculated as (7A inclusion)/(7A inclusion + 7A skipping) × 100.

Immunofluorescence. Frozen sections (6 μm thick) of unfixed TA muscles were immunostained with an affinity-purified rabbit polyclonal anti-Clcn1 antibody (dilution 1 : 50; Alpha Diagnostics International, San Antonio, TX, USA). The secondary antibody was Alexa Fluor 488-conjugated goat anti-rabbit IgG (Life Technologies) used at a dilution of 1 : 600. Images were collected using an IX70 inverted microscope (Olympus, Tokyo, Japan) equipped with a ×20 objective lens. Exposure time and threshold were identical for all comparisons of antisense and saline controls.

Statistics. A two-tailed Student's *t*-test or Tukey's multiple comparison test were used for statistical comparison.

1. Aslanidis, C. *et al.* Cloning of the essential myotonic dystrophy region and mapping of the putative defect. *Nature* **355**, 548–551 (1992).
2. Brook, J. D. *et al.* Molecular basis of myotonic dystrophy: expansion of a trinucleotide (CTG) repeat at the 3′ end of a transcript encoding a protein kinase family member. *Cell* **68**, 799–808 (1992).
3. Buxton, J. *et al.* Detection of an unstable fragment of DNA specific to individuals with myotonic dystrophy. *Nature* **355**, 547–548 (1992).
4. Harley, H. G. *et al.* Expansion of an unstable DNA region and phenotypic variation in myotonic dystrophy. *Nature* **355**, 545–546 (1992).
5. Harper, P. S. *Myotonic dystrophy,* 3rd ed. (Saunders, W. B. Philadelphia, 2001).
6. Philips, A. V., Timchenko, L. T. & Cooper, T. A. Disruption of splicing regulated by a CUG-binding protein in myotonic dystrophy. *Science* **280**, 737–741 (1998).
7. Savkur, R. S., Philips, A. V. & Cooper, T. A. Aberrant regulation of insulin receptor alternative splicing is associated with insulin resistance in myotonic dystrophy. *Nat. Genet.* **29**, 40–47 (2001).
8. Fugier, C. *et al.* Misregulated alternative splicing of BIN1 is associated with T tubule alterations and muscle weakness in myotonic dystrophy. *Nat. Med.* **17**, 720–725 (2011).
9. Koebis, M. *et al.* Alternative splicing of myomesin 1 gene is aberrantly regulated in myotonic dystrophy type 1. *Genes Cells* **16**, 961–972 (2011).
10. Ohsawa, N., Koebis, M., Suo, S., Nishino, I. & Ishiura, S. Alternative splicing of PDLIM3/ALP, for alpha-actinin-associated LIM protein 3, is aberrant in persons with myotonic dystrophy. *Biochem. Biophys. Res. Commun.* **409**, 64–69 (2011).
11. Charlet, B. N. *et al.* Loss of the muscle-specific chloride channel in type 1 myotonic dystrophy due to misregulated alternative splicing. *Mol. Cell.* **10**, 45–53 (2002).
12. Mankodi, A. *et al.* Expanded CUG repeats trigger aberrant splicing of ClC-1 chloride channel pre-mRNA and hyperexcitability of skeletal muscle in myotonic dystrophy. *Mol. Cell.* **10**, 35–44 (2002).
13. Lossin, C. & George, A. L. Jr. Myotonia congenita. *Adv. Genet.* **63**, 25–55 (2008).
14. Wheeler, T. M., Lueck, J. D., Swanson, M. S., Dirksen, R. T. & Thornton, C. A. Correction of ClC-1 splicing eliminates chloride channelopathy and myotonia in mouse models of myotonic dystrophy. *J. Clin. Invest.* **117**, 3952–3957 (2007).
15. Kole, R., Krainer, A. R. & Altman, S. RNA therapeutics: beyond RNA interference and antisense oligonucleotides. *Nat. Rev. Drug. Discov.* **11**, 125–140 (2012).
16. Stein, D., Foster, E., Huang, S. B., Weller, D. & Summerton, J. A specificity comparison of four antisense types: morpholino, 2′-O-methyl RNA, DNA, and phosphorothioate DNA. *Antisense Nucleic Acid Drug Dev.* **7**, 151–157 (1997).
17. Wu, B. *et al.* Dose-dependent restoration of dystrophin expression in cardiac muscle of dystrophic mice by systemically delivered morpholino. *Gene Ther.* **17**, 132–140 (2010).
18. Wheeler, T. M. *et al.* Targeting nuclear RNA for in vivo correction of myotonic dystrophy. *Nature* **488**, 111–115 (2012).
19. Leger, A. J. *et al.* Systemic delivery of a peptide-linked morpholino oligonucleotide neutralizes mutant RNA toxicity in a mouse model of myotonic dystrophy. *Nucleic Acid Ther.* **23**, 109–117 (2013).
20. Lu, Q. L., Liang, H. D., Partridge, T. & Blomley, M. J. Microbubble ultrasound improves the efficiency of gene transduction in skeletal muscle in vivo with reduced tissue damage. *Gene Ther.* **10**, 396–405 (2003).
21. Shen, Z. P., Brayman, A. A., Chen, L. & Miao, C. H. Ultrasound with microbubbles enhances gene expression of plasmid DNA in the liver via intraportal delivery. *Gene Ther.* **15**, 1147–1155 (2008).
22. Haag, P. *et al.* Microbubble-enhanced ultrasound to deliver an antisense oligodeoxynucleotide targeting the human androgen receptor into prostate tumours. *J. Steroid Biochem. Mol. Biol.* **102**, 103–113 (2006).
23. Suzuki, R. *et al.* Gene delivery by combination of novel liposomal bubbles with perfluoropropane and ultrasound. *J. Control Release* **117**, 130–136 (2007).
24. Negishi, Y. *et al.* Delivery of an angiogenic gene into ischemic muscle by novel bubble liposomes followed by ultrasound exposure. *Pharm. Res.* **28**, 712–719 (2011).
25. Negishi, Y. *et al.* Local gene delivery system by bubble liposomes and ultrasound exposure into joint synovium. *J. Drug Deliv.* **2011**, 203986 (2011).
26. Negishi, Y. *et al.* Systemic delivery systems of angiogenic gene by novel bubble liposomes containing cationic lipid and ultrasound exposure. *Mol. Pharm.* **9**, 1834–1840 (2012).
27. Sugano, M. *et al.* Gene delivery system involving Bubble liposomes and ultrasound for the efficient in vivo delivery of genes into mouse tongue tissue. *Int. J. Pharm.* **422**, 332–337 (2012).
28. Negishi, Y. *et al.* AG73-modified Bubble liposomes for targeted ultrasound imaging of tumor neovasculature. *Biomaterials* **34**, 501–507 (2013).
29. Kino, Y. *et al.* MBNL and CELF proteins regulate alternative splicing of the skeletal muscle chloride channel CLCN1. *Nucleic Acids Res.* **37**, 6477–6490 (2009).
30. Lin, X. *et al.* Failure of MBNL1-dependent post-natal splicing transitions in myotonic dystrophy. *Hum. Mol. Genet.* **15**, 2087–2097 (2006).
31. Summerton, J. & Weller, D. Morpholino antisense oligomers: design, preparation, and properties. *Antisense Nucleic Acid Drug Dev.* **7**, 187–195 (1997).
32. Templeton, N. S. & Templeton, N. S. *Gene and cell therapy: therapeutic mechanisms and strategies.* 2nd ed. (Marcel Dekker, New York, 2004).
33. Sazani, P. *et al.* Systemically delivered antisense oligomers upregulate gene expression in mouse tissues. *Nat. Biotechnol.* **20**, 1228–1233 (2002).
34. Chen, M. F., Niggeweg, R., Iaizzo, P. A., Lehmann-Horn, F. & Jockusch, H. Chloride conductance in mouse muscle is subject to post-transcriptional compensation of the functional Cl- channel 1 gene dosage. *J. Physiol.* **504**, 75–81 (1997).
35. Berg, J., Jiang, H., Thornton, C. A. & Cannon, S. C. Truncated ClC-1 mRNA in myotonic dystrophy exerts a dominant-negative effect on the Cl current. *Neurology* **63**, 2371–2375 (2004).
36. Ranum, L. P. & Cooper, T. A. RNA-mediated neuromuscular disorders. *Annu. Rev. Neurosci.* **29**, 259–277 (2006).

37. Wheeler, T. M. *et al.* Reversal of RNA dominance by displacement of protein sequestered on triplet repeat RNA. *Science* **325**, 336–339 (2009).
38. Mankodi, A. *et al.* Myotonic dystrophy in transgenic mice expressing an expanded CUG repeat. *Science* **289**, 1769–1773 (2000).

Acknowledgements

We thank Prof. Charles A. Thornton (University of Rochester) for providing us HSA^{LR} mice. We also thank Dr H. Mitsuhashi for valuable discussions and encouragement. This work was supported in part by the Comprehensive Research on Disability Health and Welfare, from the Ministry of Health, Labour and Welfare Japan, and Intramural Research Grant (23–5) for Neurological and Psychiatric Disorders of NCNP.

Author contributions

S.I. conceived the project. M.K. designed the experiments. T.K. carried out cell culture-based splicing assay. K.N., M.P.T. carried out the delivery of PMO. R.M., Y.H. and I.N. carried out histochemical staining. H.Y., M.H., M.S. and D.Y. designed and carried out EMG analysis. Y.N. and Y.E.-T. prepared Bubble liposomes.

Additional information

Supplementary Information accompanies this paper at http://www.nature.com/scientificreports

Competing financial interests: The authors declare no competing financial interests.

How to cite this article: Koebis, M. *et al.* Ultrasound-enhanced delivery of Morpholino with Bubble liposomes ameliorates the myotonia of myotonic dystrophy model mice. *Sci. Rep.* 3, 2242; DOI:10.1038/srep02242 (2013).